Atmospheric
Chemistry
and Physics

Chemical characterization and source identification of PM$_{2.5}$ at multiple sites in the Beijing–Tianjin–Hebei region, China

Xiaojuan Huang[1,2], **Zirui Liu**[1,3], **Jingyun Liu**[1], **Bo Hu**[1], **Tianxue Wen**[1], **Guiqian Tang**[1], **Junke Zhang**[1], **Fangkun Wu**[1], **Dongsheng Ji**[1], **Lili Wang**[1], and **Yuesi Wang**[1,3]

[1]State Key Laboratory of Atmospheric Boundary Layer Physics and Atmospheric Chemistry (LAPC), Institute of Atmospheric Physics, Chinese Academy of Sciences, Beijing, China
[2]Plateau Atmosphere and Environment Key Laboratory of Sichuan Province, School of Atmospheric Sciences, Chengdu University of Information Technology, Chengdu, China
[3]Center for Excellence in Regional Atmospheric Environment, Institute of Urban Environment, Chinese Academy of Sciences, Xiamen, China

Correspondence to: Zirui Liu (liuzirui@mail.iap.ac.cn) and Yuesi Wang (wys@mail.iap.ac.cn)

Abstract. The simultaneous observation and analysis of atmospheric fine particles (PM$_{2.5}$) on a regional scale is an important approach to develop control strategies for haze pollution. In this study, samples of filtered PM$_{2.5}$ were collected simultaneously at three urban sites (Beijing, Tianjin, and Shijiazhuang) and at a regional background site (Xinglong) in the Beijing–Tianjin–Hebei (BTH) region from June 2014 to April 2015. The PM$_{2.5}$ at the four sites was mainly comprised of organic matter, secondary inorganic ions, and mineral dust. Positive matrix factorization (PMF) demonstrated that, on an annual basis, secondary inorganic aerosol was the largest PM$_{2.5}$ source in this region, accounting for 29.2–40.5 % of the PM$_{2.5}$ mass at the urban sites; the second-largest PM$_{2.5}$ source was motor vehicle exhaust, particularly in Beijing (24.9 %), whereas coal combustion was also a large source in Tianjin (12.4 %) and Shijiazhuang (15.5 %), with particular dominance in winter. Secondary inorganic aerosol plays a vital role in the haze process, with the exception of the spring haze in Shijiazhuang and Tianjin, for which the dust source was crucial. In addition to secondary transformations, local direct emissions (coal combustion and motor vehicle exhaust) significantly contribute to the winter haze at the urban sites. Moreover, with the aggravation of haze pollution, the OC / EC mass ratio of PM$_{2.5}$ decreased considerably and the nitrate-rich secondary aerosol increased during all four seasons in Beijing, both of which indicate that local motor vehicle emissions significantly contribute to the

severe haze episodes in Beijing. To assess the impacts of regional transport on haze pollution, the PMF results were further processed with backward-trajectory cluster analysis, revealing that haze pollution usually occurred when air masses originating from polluted industrial regions in the south prevailed and is characterized by high PM$_{2.5}$ loadings with considerable contributions from secondary aerosols. This study suggests that control strategies to mitigate haze pollution in the BTH region should focus on the reduction of gaseous precursor emissions from fossil fuel combustion (motor vehicle emissions in Beijing and coal combustion in Tianjin, Hebei, and nearby provinces).

1 Introduction

Due to rapid economic development, rapid urbanization processes, and excessive energy consumption, regional haze pollution has been recognized as the most severe environmental problem in China and has received extensive attention from the government, the public, and scientists in recent years (R. Y. Zhang et al., 2015). Haze pollution mainly occurs in economically developed urban agglomerations; the most seriously polluted regions are typically the Beijing–Tianjin–Hebei (BTH) region, the Yangtze River Delta (YRD) region, the Pearl River Delta region (PRD), and the Sichuan Basin (Zhang et al., 2012; Zhang and Cao, 2015). The BTH region,

which includes the two megacities of Beijing and Tianjin as well as Hebei Province, has the highest density of coal consumption and heavily polluting industries in China. It is surrounded by Shandong, Henan, Shanxi, and Inner Mongolia, which are all heavily populated, industrialized, and urbanized and are frequently reported to have serious haze pollution due to their intensive emissions of air pollutants (Liang et al., 2016; L. T. Wang et al., 2014). Therefore, because the BTH region features the strongest pollutant emissions (Zhao et al., 2012), unfavorable meteorological conditions (Cai et al., 2017; Xu et al., 2011), and a unique topography, extreme haze pollution characterized by high fine particulate matter (PM$_{2.5}$) loading and very low visibility has frequently occurred in this region. From 2014–2015, of the 190 priority pollution monitoring cities in China, the annual average concentration of atmospheric PM$_{2.5}$ was highest in the BTH region (Zhang and Cao, 2015). Additionally, this region is characterized by frequent dust storms and corresponding high mineral-dust loading episodes in spring (Huang et al., 2010; Sun et al., 2010).

Haze pollution with high fine PM loading could profoundly impact ecosystems, regional-scale atmospheric visibility, traffic safety, the economy, and interactions with climate (R. Y. Zhang et al., 2015); more importantly, this pollution can have adverse effects on human health, including increased risks of respiratory, cardiac, and other medical conditions (Elliot et al., 2016; Wu et al., 2017), thus leading to increased mortality rates, especially in megacities, which are generally seriously polluted and densely populated. In addition to the particle mass concentration and particle size, the health effects of PM are closely related to its chemical composition (R. Y. Zhang et al., 2015), and different diseases respond variously to different air pollutants (Tang et al., 2017). Moreover, the climate and environmental domino effects of PM are also closely related to the PM chemical compositions due to their different optical properties, such as those of black carbon, mineral particles, and brown carbon, which are light absorbing, while organic matter, ammonium sulfate, and ammonium nitrate are light scattering (J. Tao et al., 2014; Y. H. Wang et al., 2015; Wu et al., 2009; Zhang et al., 2016). These chemical constituents mainly originate from various anthropogenic sources, such as coal combustion, vehicle exhaust emissions, biomass burning, cooking, and industry-related emissions, among others. Therefore, the key to reducing PM$_{2.5}$ concentrations and improving air quality is to control these sources, which necessitates a strong demand for increased knowledge about the detailed chemical natures and sources of PM$_{2.5}$ in the BTH region.

Haze pollution has significant regional characteristics. In addition to local emissions, the regional or interregional transport of primary PM and gaseous precursors plays an important role during haze periods (Chen et al., 2017; Li et al., 2017, 2015; Tao et al., 2012; L. T. Wang et al., 2014; Ying et al., 2014). For example, the SO$_2$ measured in Beijing includes a large regional contribution transported from southern industrial areas (Guo et al., 2014). This contribution points to an urgent demand for wider collaborative work on emission control strategies between neighboring cities or provinces. For Shanghai, which is a megacity in the YRD region, Wu et al. (2017) estimated that the application of multiregional integrated control strategies in neighboring provinces could be most effective in reducing PM$_{2.5}$ in Shanghai and could largely reduce the economic losses caused by haze pollution. Extensive studies have been performed to investigate the formation mechanisms and emission sources of haze pollution in the BTH region and have obtained many valuable results (Du et al., 2014; Liu et al., 2016a; Sun et al., 2013; Y. S. Wang et al., 2014; Zhang et al., 2014; X. J. Zhao et al., 2013d). Massive anthropogenic emissions from diverse local sources, such as regional civil and industrial energy consumption, urban traffic, biomass burning, and resuspended dust, and those transported from nearby provinces are widely regarded as the intrinsic factors behind regional haze pollution events (Zhang et al., 2013; Zhao et al., 2012). Abnormal and unfavorable weather conditions also act as crucial factors in the formation of extensive and prolonged haze pollution events, such as the persistent haze event in January 2013 (M. Tao et al., 2014; Y. S. Wang et al., 2014). In addition, many case studies, such as the winter regional haze events of 2010 (X. J. Zhao et al., 2013) and 2013 (Sun et al., 2014; Y. S. Wang et al., 2014), have also revealed that severe haze events are largely driven by the high secondary production of sulfate, nitrate, ammonium, and secondary organic aerosols (SOAs), suggesting that aerosol chemistry plays a dominant role in haze evolution. Recent studies have reported a new efficient formation pathway for sulfate in the Beijing winter haze via reactive nitrogen chemistry in aerosol water during haze events (Cheng et al., 2016; He et al., 2014; G. Wang et al., 2016; Y. Wang et al., 2013). In terms of haze mitigation strategies, Guo et al. (2014) suggested that regulatory controls on gaseous emissions for volatile organic compounds and nitrogen oxides from local transportation and sulfur dioxide from regional industrial sources are the keys to reducing the urban PM level in Beijing. However, these studies were often conducted at single sites (mostly in Beijing) and/or for short periods (specific haze events or a certain season); long-term multisite studies are scarce (Li et al., 2017; Shen et al., 2016; Zhang et al., 2013; Zhao et al., 2013c; Zong et al., 2016). In such studies, further questions are raised. First, due to the relatively few studies in Tianjin and Hebei, especially with respect to source explorations of PM$_{2.5}$, we cannot fully understand the overall characteristics of the haze pollution in the BTH region. Second, it is hard to directly compare the results between single-site studies to conduct a regional assessment as these studies covered different time periods and were conducted using different analytical approaches. Third, the spatial and temporal variability of the PM$_{2.5}$ sources in this region have not been extensively investigated, particularly with respect to the evolution of emission sources at dif-
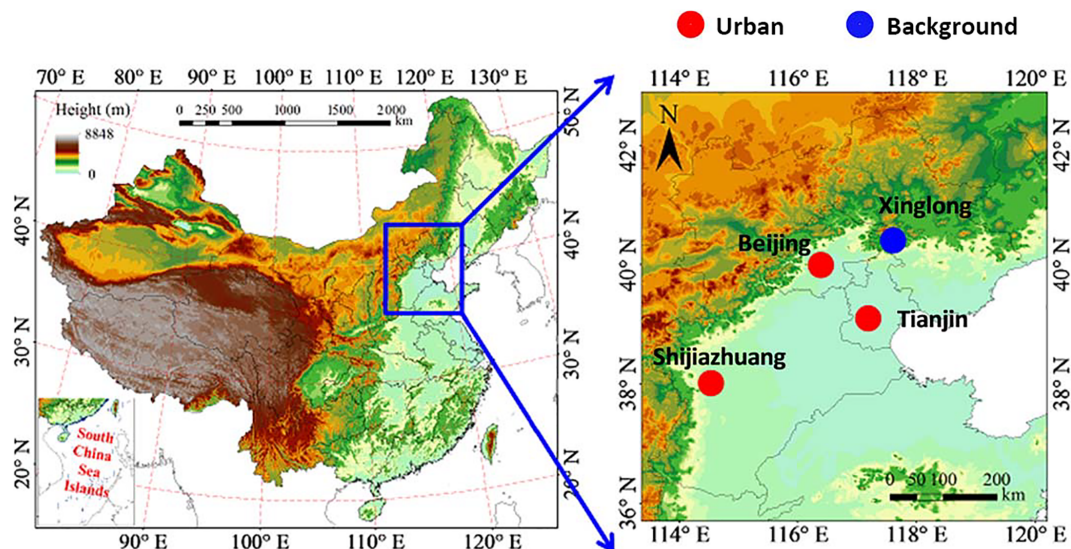
Figure 1. Map of the sampling sites (Beijing, Tianjin, and Shijiazhuang are representative of urban stations, whereas Xinglong represents the regional background).

ferent pollution levels and their spatial variability. The above imperfections can limit the understanding of the sources and evolution processes of haze pollution on a regional scale and complicate effective mitigation strategies.

In this study, we conducted simultaneous measurements of PM$_{2.5}$ at three urban sites (Beijing, Tianjin, Shijiazhuang) in the BTH region and at one regional background site (Xinglong) and analyzed their chemical compositions and quantified the apportionment of their sources using unified data processing and analytical methods. In addition, we emphatically analyzed the evolution of the chemical compositions and emission sources at different pollution levels and their seasonal and spatial differences. To further explore the influences of regional transport on haze pollution, the source apportionment results in combination with the backward-trajectory clustering were used. This study can provide an overall understanding of the regional signal of PM$_{2.5}$ pollution in the BTH region and support stakeholders and policy makers in understanding the impacts of regional sources on high PM$_{2.5}$ loadings, thus facilitating the design of effective joint emission abatement strategies.

2 Materials and methods

2.1 Sites and sampling

2.1.1 Site description

Four sampling sites were selected in the Beijing–Tianjin–Hebei region (Fig. 1), including three urban sites (Beijing, Tianjin, and Shijiazhuang) and a regional background site (Xinglong). Beijing is the capital of China, Tianjin is an economically developed municipality, and Shi-

jiazhuang is the capital of Hebei Province with an annual PM$_{2.5}$ concentration in 2013 ranking second in Hebei Province and the whole of China (http://www.greenpeace.org.cn/PM25-ranking/). These three cities have their own atmospheric characteristics due to their different energy and industrial structures and could thus represent the pollution characteristics of different types of urban areas in the BTH region. The Beijing site (39.97° N, 116.38° E) was situated in the courtyard of the Institute of Atmospheric Physics (IAP) of the Chinese Academy of Sciences (CAS). The Tianjin site (39.09° N, 117.19° E) was located in the Tianjin Atmospheric Boundary Layer Observatory of the Chinese Meteorological Administration, and the Shijiazhuang site (38.03° N, 114.53° E) was located at the Hebei Meteorological Service. The sampling sites in Beijing, Tianjin, and Shijiazhuang were affected by nonspecific pollution sources while being influenced by mixed emission sources, such as local motor vehicle emissions, coal combustion, road dust, industrial activities, cooking, and transported pollutants. Therefore, these sites are considered to be representative of typical urban environments. The sampling site in Xinglong (40.39° N, 117.58° E) was located at Xinglong Observatory, National Astronomical Observatory, Chinese Academy of Sciences. Xinglong Observatory is located in the northeastern region of Beijing with a distance of approximately 110 km from Beijing and is surrounded by mountains, thus allowing it to be minimally affected by human activities. Therefore, it is one of the regional atmospheric background stations of the Chinese Academy of Sciences.

2.1.2 PM$_{2.5}$ sampling

The PM$_{2.5}$ samples were simultaneously collected at the four sites using a PM$_{2.5}$ sampler (TH-150C; Wuhan Tianhong, China) at an airflow rate of 100 L min^{-1} from June 2014 to April 2015. During each season, we collected PM$_{2.5}$ samples on 90 mm quartz membrane filters every day and night for 1 month, except on rainy days. The specific sampling period for the summer extended from 15 June to 14 July 2014, that of the autumn extended from 15 September to 14 October 2014, that of the winter extended from 29 December 2014 to 27 January 2015, and that of the spring extended from 20 March to 18 April 2015. The sampling time of each sample was 11.5 h, which generally occurred from 08:00 to 19:30 during the daytime and from 20:00 to 07:30 of the next day during the night. Over the entire observational period, 224, 214, 221, and 211 samples were collected in Beijing, Tianjin, Shijiazhuang, and Xinglong, respectively, and the numbers of samples in each season are shown in Table S1 in the Supplement.

Detailed records of the instrumental conditions were collected during the sampling, including the sampling time, the sampled air volume, atmospheric pressure, and air temperature. After sampling, the quartz filters were individually placed in petri dishes and immediately stored at −20 °C prior to weighing and subsequent analysis. To ensure that the instrument worked at the specified flow rate, the airflow rate of the sampler was calibrated before and after each sampling. The carbon brush was replaced every month, and the outlet of the tail pipe was kept far away from the sampler in order to avoid contaminating the filter samples. During the sampling process, strict quality control was conducted to avoid any contamination. The frequent cleaning of the cutter and tray of the membrane was necessary.

2.2 Filter analysis

2.2.1 Gravimetry

The quartz membrane filters, which were packaged with aluminum foil, were prefired in a muffle furnace at 500° for 4 h to remove organic material. In addition, in order to minimize the influence of water adsorption, the filters were weighed before and after sampling using a microelectronic balance with a reading precision of 10 μg after undergoing a 48 h equilibration period inside a chamber under the conditions of constant temperature (20 ± 1°) and humidity (45 ± 5 %). The atmospheric PM$_{2.5}$ masses were deduced from the gravimetric measurements performed before and after sampling. To guarantee the accuracy of the weights, the weighing was repeated until a difference of less than 0.10 mg between the two measured weights was achieved. All the procedures were strictly quality controlled to avoid any possible contamination of the samples.

2.2.2 Chemical analysis

A size of 2.011 cm^2 filter split from one-quarter of each sample was ultrasonically extracted using 50 mL of deionized water (with a specific resistivity of 18.2 MΩ cm^{-1}) for 30 min. After passing through microporous membranes with pore sizes of 0.22 μm, the extracted solutions were analyzed using an ion chromatograph (IC) system (ICS-90; Dionex, USA) for the detection of SO$_4^{2-}$, NO$_3^-$, NH$_4^+$, Cl$^-$, K$^+$, Na$^+$, Ca^{2+}, and Mg^{2+}. More details are given in Huang et al. (2016).

A 0.495 cm^2 punch from another quarter of each sample was used for the analysis of organic carbon (OC) and elemental carbon (EC), which was performed using a thermal/optical carbon aerosol analyzer (DRI model 2001A; Desert Research Institute, USA) following the protocol of IMPROVE_A (TOR). In a pure helium atmosphere, OC1, OC2, OC3, and OC4 are produced stepwise at 140, 280, 480, and 580°, respectively, followed by EC1 (540°), EC2 (780°), and EC3 (840°) in a 2 % oxygen-contained helium atmosphere. The OPC (organic pyrolyzed carbon) is determined when the reflected laser signal returns to its initial value after oxygen is added to the analyzed atmosphere. Therefore, OC is operationally defined as OC = OC1 + OC2 + OC3 + OC4 + OPC, while EC is defined as EC = EC1 + EC2 + EC3–OPC. Detailed procedures can be found in Xin et al. (2015).

The microwave acid digestion method was used to digest the filter samples into a liquid solution for elemental analysis. One-quarter of each filter sample was placed in the digestion vessel with a mixture of 6 mL HNO$_3$, 2 mL H$_2$O$_2$, and 0.6 mL HF and was then exposed to a three-stage microwave digestion procedure from a microwave-accelerated reaction system (MARS; CEM Corporation, USA). After that, the digestion solution was transferred to PET bottles and diluted to 50 mL with deionized water (with a conductivity of 18.2 MΩ cm^{-1}). Inductively coupled plasma mass spectrometry (ICP-MS 7500a; Agilent Technologies, Japan subsidiary) was used to determine the concentrations of 18 trace elements in the digestion solution, including Mg, Al, K, Ca, V, Cr, Mn, Fe, Co, Ni, Cu, Zn, As, Se, Ag, Cd, Tl, and Pb. More detailed information, such as instrument optimization, calibration, and quality control, is given in J. Wang et al. (2016).

2.3 Data analysis method

2.3.1 Chemical mass closure

The chemically reconstructed PM$_{2.5}$ mass (PM$_{chem}$) was calculated as comprised of eight categories of chemical species,

which can be expressed as follows:

$$[PM_{chem}] = [Organic\ matter] + [EC] + [Mineral\ dust]$$
$$+ [Trace\ metals] + [Sulfate] + [Nitrate]$$
$$+ [Ammonium] + [Chloride]. \qquad (1)$$

In estimating organic matter (OM), an OC to OM conversion factor of 1.6 was adopted for the aerosols at urban sites (Cao et al., 2007; Turpin and Lim, 2001) and the regional background site. Although the literature suggests that a higher OC to OM conversion factor of 2.1 is suitable for rural sites (Bressi et al., 2013; Turpin and Lim, 2001), we still used a uniform value of 1.6 for the sake of spatial comparisons. Therefore,

$$[OM] = 1.6 \times [OC]. \qquad (2)$$

The calculation of mineral dust was performed on the basis of crustal element oxides (such as Al_2O_3, SiO_2, CaO, Fe_2O_3, TiO_2, MnO_2, and K_2O; Christoforou et al., 2000). The Ti content was very low in atmospheric particulate matter, with $0.04\ \mu g\ m^{-3}$ measured in the PM$_{2.5}$ in Beijing, Tianjin, and Shijiazhuang (Zhao et al., 2013b). Thus, eliminating the Ti content has an almost negligible influence on the estimation of the mineral dust. Mineral dust was calculated as follows:

$$[Mineral\ dust] = [Al_2O_3] + [SiO_2] + [CaO] + [MnO_2]$$
$$+ [Fe_2O_3] + [K_2O] = 2.14 \times [Si]$$
$$+ 1.89 \times [Al] + 1.4 \times [Ca] + 1.58 \times [Mn]$$
$$+ 1.43 \times [Fe] + 1.21 \times [K]. \qquad (3)$$

In this study, the measurements of the trace elements in the particles did not include the determination of Si, so the Si content was calculated based on its ratio to Al in crustal materials: $[Si] = 3.41 \times [Al]$ (Mason, 1966). The calculations of K_2O and Fe_2O_3 were also based on their ratios to Al in crustal materials (Wedepohl, 1995) since they have abundant artificial sources in addition to natural sources.

The trace metal content reflects the sum of 11 different heavy metal species and is expressed as

$$[Trace\ metals] = V + Co + Ni + Cu + Pb + Zn + As$$
$$+ Se + Ag + Cd + Tl. \qquad (4)$$

The above chemical reconstruction method was applied to the four sites, and comparisons of the reconstructed results (PM$_{chem}$) with the gravimetric results (PM$_{grav}$) are shown in the Supplement Fig. S1. It can be clearly seen that PM$_{chem}$ is significantly related to PM$_{grav}$, indicating that the chemical reconstruction method exhibited strong reliability. However, the PM$_{chem}$ concentrations at the four sites were all less than those of PM$_{grav}$; therefore, there is unresolved matter that may largely be retaining water in the sampling membrane and particulate matter. Moreover, during the period between weighing and chemical measurements, the volatilization of organic matter and the decomposition of ammonium nitrate may occur. The discrepancy between PM$_{chem}$ and PM$_{grav}$ was thus defined as unknown.

2.3.2 Source apportionment

The EPA Positive Matrix Factorization (PMF) 5.0 model was applied to apportion the sources of PM$_{2.5}$ in this study, as it is an effective source apportionment receptor model that has been successfully applied for source apportionments in many cities and regions worldwide (Huang et al., 2014; Reff et al., 2007). Unlike to the CMB model (chemical mass balance), the PMF model does not require source profiles prior to analysis but only requires the values of the concentrations of the sample species and their uncertainties (US Environmental Protection Agency, 2014; Y. J. Zhang et al., 2015). In this study, the model simulations were applied to data sets comprised of 34 species: eight carbon fractions (OC1, OC2, OC3, OC4, OPC, EC1, EC2, and EC3), 8 inorganic species (SO_4^{2-}, NO_3^-, NH_4^+, K^+, Na^+, Ca^{2+}, Mg^{2+}, and Cl^-), and 18 trace elements (Mg, Al, K, Ca, V, Cr, Mn, Fe, Co, Ni, Cu, Zn, As, Se, Ag, Cd, Tl, and Pb). Due to the low OC and EC concentrations at the background site, the entire concentrations of OC and EC were input into the PMF model instead of the eight carbon fractions. In addition to the concentrations of the sample chemical species, the uncertainties in the sample species were calculated based on two different situations according to the PMF 5.0 user guide (US Environmental Protection Agency, 2014).

If the concentration is less than or equal to the provided method detection limit (MDL), the uncertainty is calculated using a fixed fraction of the MDL, which is written as Uncertainty $= \frac{5}{6}$ MDL. If the concentration is greater than the provided MDL, the calculation is defined as Uncertainty $= \sqrt{(Error\ Fraction + Concentrtion)^2 + (0.05\ MDL)^2}$. In this study, the error fractions of SO_4^{2-}, NO_3^-, and NH_4^+ were estimated to be 5 %. Those of OPC, EC2, and EC3 were 15 %, and those of other species were 10 %. PMF analysis requires a complete data set; in order to reduce the error, the samples with missing values for individual species were excluded rather than replaced by the mean concentrations of the remaining observations.

The number of factors must be chosen prior to using PMF. In this study, the PMF solutions using 5–12 factors at the three urban sites and 3–9 factors at the regional background site were explored with a final factor number chosen based on interpretability and stability across bootstrap-replicate data sets (Xie et al., 2013a, b).

2.4 Meteorological data and backward-trajectory modeling

Meteorological data, including the ambient temperature, relative humidity, and wind speed in Beijing and Xinglong, were measured within 50 m of the filter sampling sites, using an automatic meteorological observation instrument (Milos520; Vaisala, Finland) located at an 8 m measurement height. In addition, in Tianjin and Shijiazhuang, the meteorological data were obtained from the meteorological mon-

itoring stations of the China Meteorological Administration, which was located within 100 m of the sampling sites.

The backward-trajectory analysis method is widely applied to identify the potential source regions and transport pathways of air masses, especially for serious air pollution episodes (Gao et al., 2015; Hu et al., 2012; Zhang et al., 2014). In this study, 48 h backward trajectories terminated at a height of 100 m above ground level were calculated for the four sampling sites using the Hybrid Single-Particle Lagrangian Integrated Trajectory (HYSPLIT 4.9) model developed by the US National Oceanic and Atmospheric Administration Air Resources Laboratory (NOAA ARL). The trajectories were calculated every 12 h with starting times at 08:00 and 20:00 local time (corresponding to each sampling) during the entire observational period.

3   Results and discussion

3.1   General characteristics of PM$_{2.5}$

3.1.1   Annual mass concentrations

The temporal variability in the gravimetrically determined PM$_{2.5}$ concentrations at the four sites (Beijing, Tianjin, Shijiazhuang, and Xinglong) throughout the entire observation period is shown in Fig. 2. The strong day-to-day variability in the PM$_{2.5}$ concentrations can be easily observed, especially in winter when PM$_{2.5}$ concentrations range from 34.1 to 612.6 µg m^{-3} in Shijiazhuang. These concentrations typically record periodic "clean–polluted–clean" cycles for a few days, which were also reported by Guo et al. (2014), who noted that the Beijing haze pollution underwent clear periodic cycles of 4–7 days in length. These periodic cycles of haze episodes are primarily driven by atmospheric processes and fluctuations in meteorological conditions (Guo et al., 2014; R. Y. Zhang et al., 2015), such as wind speed, relative humidity, air temperature and pressure, atmospheric stability, the height of the planetary boundary layer, and air mass origins. Very similar patterns of PM$_{2.5}$ temporal variations were found at all four sites (Fig. 2), suggesting homogeneous characteristics of atmospheric particulate matter on a regional scale.

On average, the annual PM$_{2.5}$ concentrations throughout the entire observation period recorded higher levels at the urban sites, which were 99.5 ± 67.4, 105.7 ± 63.1, and 155.2 ± 100.8 µg m^{-3} in Beijing, Tianjin, and Shijiazhuang, respectively, representing values that were 1.5, 1.6, and 2.4 times those at the background site (Xinglong), respectively. During the entire observational period, 81 % of the samples in Shijiazhuang exceeded the second grade of the PM$_{2.5}$ daily average mass concentrations in China (75 µg m^{-3}), followed by Tianjin (63 %) and Beijing (55 %), with the minimum occurring in Xinglong (29 %; Table S1). Particularly serious pollution was observed in Shijiazhuang, which consumes

huge amounts of energy for industrial processes and daily life (Zhao et al., 2013c) and exhibits higher relative humidity and lower wind speeds than the other sites (Table S2), which are both beneficial for the accumulation of PM$_{2.5}$ mass (T. T. Liu et al., 2017). Moreover, the largest differences in the PM$_{2.5}$ average mass concentrations between the urban sites and the background site occurred in winter, yielding values 2.2–4.1 times those in Xinglong. This spatial difference can be explained by the strong intensity of pollution emissions (coal combustion for heating) in winter at the urban sites.

3.1.2   Seasonal variation

Due to the minor effects of anthropogenic emissions, the seasonal variations in PM$_{2.5}$ concentrations in Xinglong were not significant (56.7–77.9 µg m^{-3}), and only slightly higher values were observed in spring. Zhao et al. (2009) also determined that the maximum PM$_{2.5}$ concentrations usually occur in spring in Shangdianzi, which is another regional background area in the North China Plain. However, at the urban sites, significant seasonal variations were observed, especially in Shijiazhuang. The highest PM$_{2.5}$ values were recorded in winter, with average concentrations of 124.8 ± 69.9, 136.6 ± 93.8, and 231.8 ± 129.1 µg m^{-3} in Beijing, Tianjin, and Shijiazhuang, respectively. There were four extreme haze episodes that occurred in Shijiazhuang, with particularly serious episodes from 2 to 6 January and from 11 to 16 January. Numerous studies have also revealed that the heaviest haze pollution events with extremely high PM$_{2.5}$ loadings occurred in winter in the BTH region (L. Wang et al., 2012; Zhang and Cao, 2015; X. J. Zhao et al., 2013), which has mainly been attributed to the combination of intensive coal-fired heating and unfavorable meteorological conditions (i.e., more frequent occurrences of stagnant weather, temperature inversions, and low boundary layer heights) in this region (Tang et al., 2016a; Zhang and Cao, 2015; Zhao et al., 2009). Following winter, the average PM$_{2.5}$ concentrations in spring also remained at a relative high level at the urban sites (101.0–148.4 µg m^{-3}), which may have partly resulted from the enhanced mineral dust (see Fig. 4) produced by the relatively high wind speeds during this season (Table S2). Due to the strong turbulence that occurs under conditions of strong radiation intensity and high temperature in summer, as well as the high atmospheric mixing layer generally observed in this season (Tang et al., 2016a), air pollutants could have been effectively diluted and diffused, thus resulting in the lowest PM$_{2.5}$ concentrations being measured during this season. The PM$_{2.5}$ concentrations in autumn were close to those in summer, but one extreme haze episode was recorded from 5 to 11 October in Beijing and Shijiazhuang, with the highest concentration of the daily PM$_{2.5}$ reaching 394 µg m^{-3} in Beijing and 460 µg m^{-3} in Shijiazhuang. The extreme haze episode in October 2014 was recorded and analyzed in depth by Yang et al. (2015).
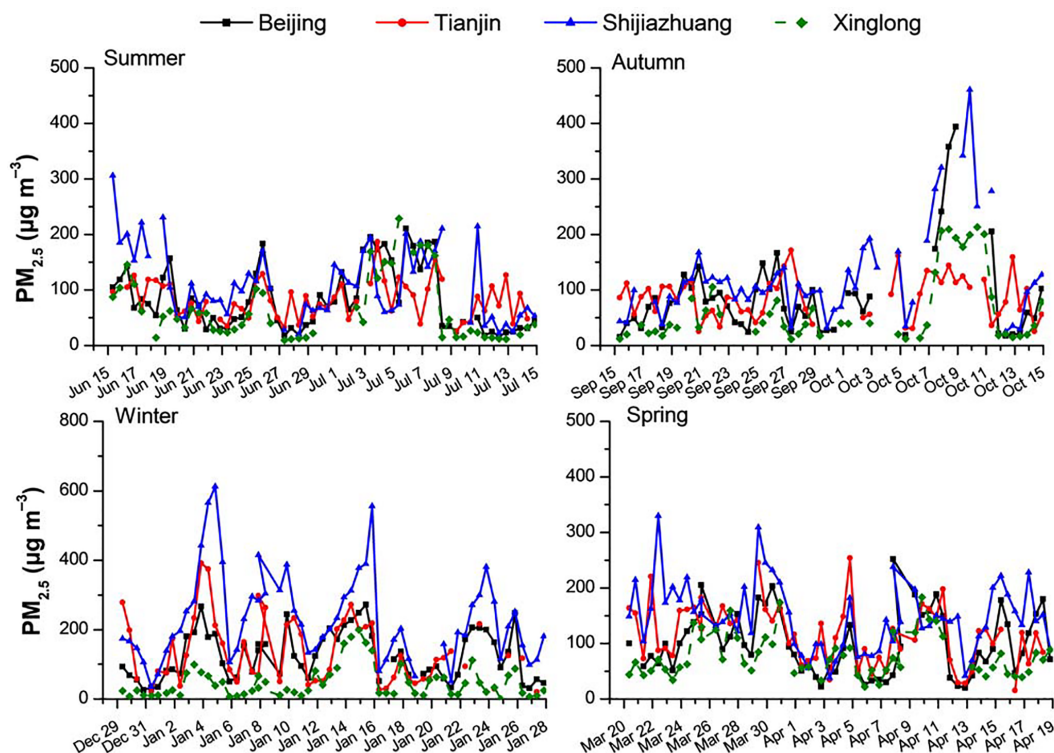
Figure 2. Time series of the gravimetric PM$_{2.5}$ concentrations during the four study periods.

3.2 Chemical compositions of PM$_{2.5}$

3.2.1 Annual compositions

The chemical compositions of the entire sample set collected from the three urban sites and the regional background site were similar, further confirming the regional homogeneity of atmospheric PM$_{2.5}$. The PM$_{2.5}$ in this region (Fig. 3) is primarily comprised of organic matter (OM = OC × 1.6, 16.0–25.0 %), secondary inorganic ions (SNA, including sulfate, nitrate, and ammonium, 43.6–53.3 %), mineral dust (14.7–20.8 %), and lower proportions of EC (2.8–6.2 %), chloride (1.9–5.5 %), and trace metals (0.4–0.6 %). The annual average concentrations of carbonaceous aerosols (OM plus EC) were 31.1, 27.0, and 44.2 μg m^{-3} in Beijing, Tianjin, and Shijiazhuang, respectively, thus constituting large fractions (25.5–31.2 %) of PM$_{2.5}$ in the urban atmosphere. It is worth noting that EC accounted for 6.2, 5.9, and 5.7 % of the measured masses of PM$_{2.5}$ in Beijing, Tianjin, and Shijiazhuang, respectively, which were higher than that measured in Xinglong (2.8 %), reflecting the strong emissions from fossil fuel combustion in urban areas. In Xinglong, lower concentrations and lower fractions of OM but higher fractions of mineral dust and SNA than at the urban sites were discovered. The presence of lower contributions of OM but higher contributions of SNA at the background site is consistent with the results measured on Qimu Island (another regional background site in northern China, which is located approx-

imately 300 km southeast of the BTH region; Zong et al., 2016). This was mainly attributed to the regional-scale emission characteristics of gaseous precursors in this region, in which there are more abundant SO$_2$, NO$_x$, and NH$_3$ emissions than OC emissions (Zhao et al., 2012), and the general characteristics of the regional atmosphere are well reflected at the regional background site.

As the key PM$_{2.5}$ constituents, sulfate, nitrate, and ammonium (SNA) are generally recognized to originate from the secondary conversions of gaseous SO$_2$, NO$_x$, and NH$_3$ via gas-phase chemical reactions and heterogeneous reactions (G. Wang et al., 2016; R. Y. Zhang et al., 2015). In this study, they accounted for 14.4–20.6, 15.1–19.6, and 11.6–13.1 % of the annual average PM$_{2.5}$ concentrations, respectively. Among the three urban sites, the highest NO$_3^-$ contribution (18.0 %) was found in Beijing, which agrees well with it having a strong traffic source. In addition, from the annual results, the mass ratio of NO$_3^-$ / SO$_4^{2-}$ in Beijing was 1.25, which was higher than that in Tianjin (0.97), Shijiazhuang (0.92), and Xinglong (0.95). The NO$_3^-$ / SO$_4^{2-}$ mass ratio has often been used as an indicator of the relative contributions of sulfur and nitrogen from mobile versus stationary sources to aerosol particles in the atmosphere (Arimoto et al., 1996; Cao et al., 2009; Han et al., 2016), as vehicle exhaust and coal combustion emissions are significant contributors of nitrate and sulfate, respectively (Huang et al., 2014). Therefore, the higher NO$_3^-$ / SO$_4^{2-}$ mass ratio in Beijing implies
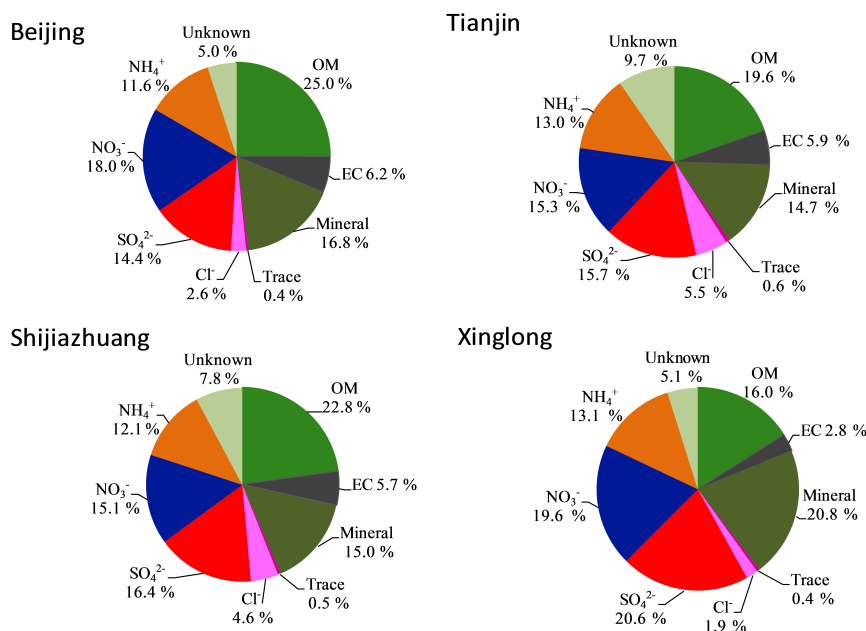
Figure 3. Pie charts depicting the percentages of the major chemical components in gravimetric PM$_{2.5}$ based on annual data.

the predominance of motor vehicle emissions in the contributions to PM pollution (Han et al., 2016; Yang et al., 2015), while in Tianjin and Shijiazhuang, coal combustion may still play a dominant role. However, compared to the reported results, the NO$_3^-$ / SO$_4^{2-}$ mass ratios of the two cities also increased from 0.85 (2009–2010; Zhao et al., 2013b) to 0.92 (this study) in Shijiazhuang and from 0.69 (2008; Gu et al., 2011) to 0.75 (2009–2010; Zhao et al., 2013b) and 0.97 (this study) in Tianjin. This increasing trend also occurred in the background area, as the NO$_3^-$ / SO$_4^{2-}$ mass ratio in Xinglong increased from 0.78 (2009–2010; Li et al., 2013) to 0.95 (this study). These results clearly revealed that atmospheric nitrate pollution is worsening in this region, which is generally recognized as being caused by increasing motor vehicle emissions and indicates the remarkable effect of the control measures on SO$_2$ emissions.

In addition to carbonaceous and SNA aerosols, mineral dust was also a major component of PM$_{2.5}$, constituting a smaller fraction of the PM$_{2.5}$ masses (14.7–16.8 %) at the urban sites than at the background site (20.8 %). Cl$^-$ exhibited higher concentrations and fractions in Shijiazhuang (7.2 µg m^{-3}, 4.6 %) and Tianjin (5.8 µg m^{-3}, 5.5 %) than it did in Beijing (2.6 µg m^{-3}, 2.6 %) and Xinglong (1.2 µg m^{-3}, 1.9 %), further illustrating the important contribution of coal combustion emissions to the PM$_{2.5}$ concentrations in Shijiazhuang and Tianjin. The concentration of trace metals varied from 0.3 to 0.7 µg m^{-3} and constituted only a minor fraction of the masses.

3.2.2   Seasonal variations

The PM mass and its chemical compositions are governed by chemical processes, the evolution of emission sources, and meteorological conditions (Bressi et al., 2013; T. T. Liu et al., 2017), which usually exhibit seasonality. The seasonal patterns of PM$_{2.5}$ at the urban sites were mainly driven by OM, SNA, and mineral dust, which were the major components of PM$_{2.5}$ during each season. In winter, the dominant component at the urban sites was OM; moreover, Fig. 4 shows that the OM concentration and its contribution to PM$_{2.5}$ mass were significantly higher in winter (38.1–82.7 µg m^{-3}, 27.9–35.7 %) than in other seasons. In addition, the EC concentration also reached a maximum value in winter at the urban sites, yielding values of 11.8, 10.7, and 16.3 µg m^{-3} in Beijing, Tianjin, and Shijiazhuang, respectively. Similar seasonal variations in carbonaceous aerosols were also observed in the BTH region (Beijing, Tianjin, Shijiazhuang, Chengde, and Shangdianzi; Zhao et al., 2013a), Jinan (Yang et al., 2012), and the Pearl River Delta region (Cao et al., 2004). There are two possible explanations for this phenomenon. On the one hand, a substantial increase in the amount of coal fires used for residential heating in winter could increase the abundance of carbon-containing emissions, including primary organic carbon, EC, and VOCs (Zhao et al., 2012). On the other hand, the lower temperatures in winter could favor the conversion from gaseous VOCs to their particulate forms (G. Wang et al., 2015), whereas the high temperatures in warm seasons, especially those in summer (during which the lowest OM concentrations can be seen in Fig. 4), may cause
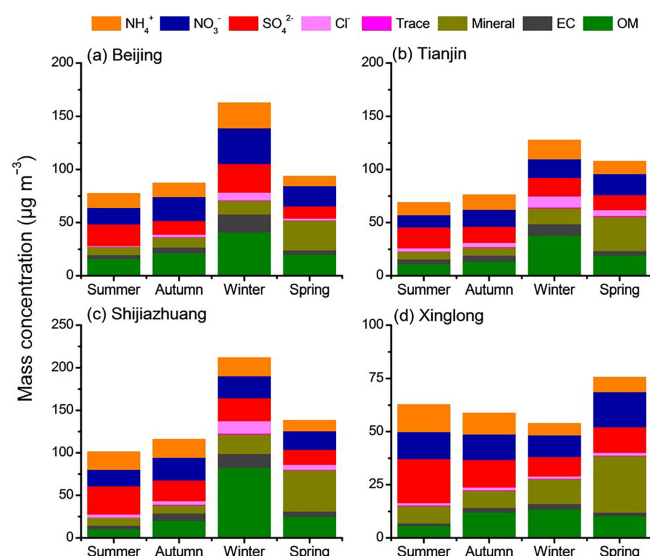
Figure 4. Seasonal variations in the major chemical components of PM$_{2.5}$ at the four sites.

the semivolatile organic compounds to mainly exist in their gaseous forms in the atmosphere. Cl$^-$, which is a good tracer of coal combustion, also exhibited higher concentrations and contributions to the PM$_{2.5}$ mass in winter (5.3–14.6 µg m^{-3}, 4.6–6.3 %) than it did in other seasons (1.0–5.6 µg m^{-3}, 1.2–4.9 %) at the urban sites. However, since it is less affected by local anthropogenic sources, the Xinglong site recorded the lowest concentrations and contributions of EC and Cl$^-$, which showed no distinct seasonal variations.

Unlike OM, SNA has its highest contributions in summer at the urban sites (51.7–66.2 %), which were significantly higher than those in winter and spring. The prominence of SNA in summer was more apparent in Xinglong (71.2 %), which reflects the dominant contributions of meteorological factors. At the urban sites, SNA also presented prominent contributions to the PM$_{2.5}$ in autumn (51.9–58.1 %), and the average PM$_{2.5}$ concentrations were comparable in summer and autumn. This may have resulted from the high relative humidity in autumn, which is even higher than that in summer (Table S2). However, the contributions of sulfate and nitrate exhibited obvious seasonal differences at these three urban sites and even more apparent differences at the background site, with greater contributions of sulfate in summer (23.6–29.9 %) and nitrate in autumn (18.4–25.7 %). This pattern was also found in our previous study in Beijing (Huang et al., 2016). This trend is closely related to the respective chemical and physical properties and mechanisms of generation, as nitrate tends to be decomposed under high temperatures (which mainly occurs in summer) due to the thermodynamic instability of ammonium nitrate, while the process of the chemical generation of ammonium sulfate (i.e., the gasphase oxidation of SO$_2$ and its subsequent heterogeneous reactions) is largely promoted under the high temperatures and

intense solar radiation of summer (Huang et al., 2016; Ianniello et al., 2011; R. Y. Zhang et al., 2015).

In spring, the primary chemical component at all four sites was mineral dust, which contributed 27.5–34.1 % to PM$_{2.5}$ and was significantly higher than it was in other seasons (7.5–20.7 %), thus reflecting the important influence of northwest dust transport on the atmospheric fine particles of the BTH region in that spring and the increase in local resuspended dust (such as road dust and construction dust) resulting from the enhanced wind speeds during this season (Table S2).

3.3 Source apportionment using PMF

The source factors of PM$_{2.5}$ were apportioned by applying the PMF receptor model at three urban sites and at the background site for comparison. The identification of the sources was based on certain chemical tracers that are generally presumed to be emitted by specific sources and are present in significant amounts in the collected samples (Singh et al., 2016). Based on this, eight factors were identified for Beijing and Tianjin, nine were identified for Shijiazhuang, and only five were identified for Xinglong. The relative dominances of each source varied by site and season. The contributions of the identified sources determined by analyzing the annual data are shown in Fig. 6; the factor profiles of PM$_{2.5}$ for the regional background site (Xinglong) are listed in Fig. 5, while those for the urban sites are shown in Figs. S2–4. These factors can be summarized as follows.

Coal combustion. In China, coal combustion is generally used in thermal power plants, for industrial fuel use, and for winter residential heating in its northern cold regions. This source is characterized by high loadings of OC, EC, and chloride, most of which were apportioned in this factor (Figs. S2–4a). At the three urban sites, the coal combustion source exhibited significantly higher contributions to the PM$_{2.5}$ (14.1, 23.3, and 29.2 % in Beijing, Tianjin, and Shijiazhuang, respectively) in winter than were seen in other seasons (0.7–10.7 %). This was strongly aligned with the seasonal characteristics of coal combustion activities in this region. The annual average emissions from coal combustion contributed only 5.6 % to the PM$_{2.5}$ in Beijing and were much higher in Tianjin (12.4 %) and Shijiazhuang (15.5 %) but were not identified at Xinglong.

Secondary aerosol and inorganic aerosol. The dominant source was secondary inorganic aerosol at the three urban sites (29.2–40.5 %) and secondary aerosol in Xinglong (45.1 %). In Xinglong, this factor (Fig. 5a) can be identified as secondary aerosol because of the high contributions and accumulations of OC, sulfate, nitrate, and ammonium, which caused the aerosol to include secondary inorganic aerosol (SIA) and secondary organic aerosol (SOA). In addition, approximately 30 % of the total chloride was assigned to this source, indicating that
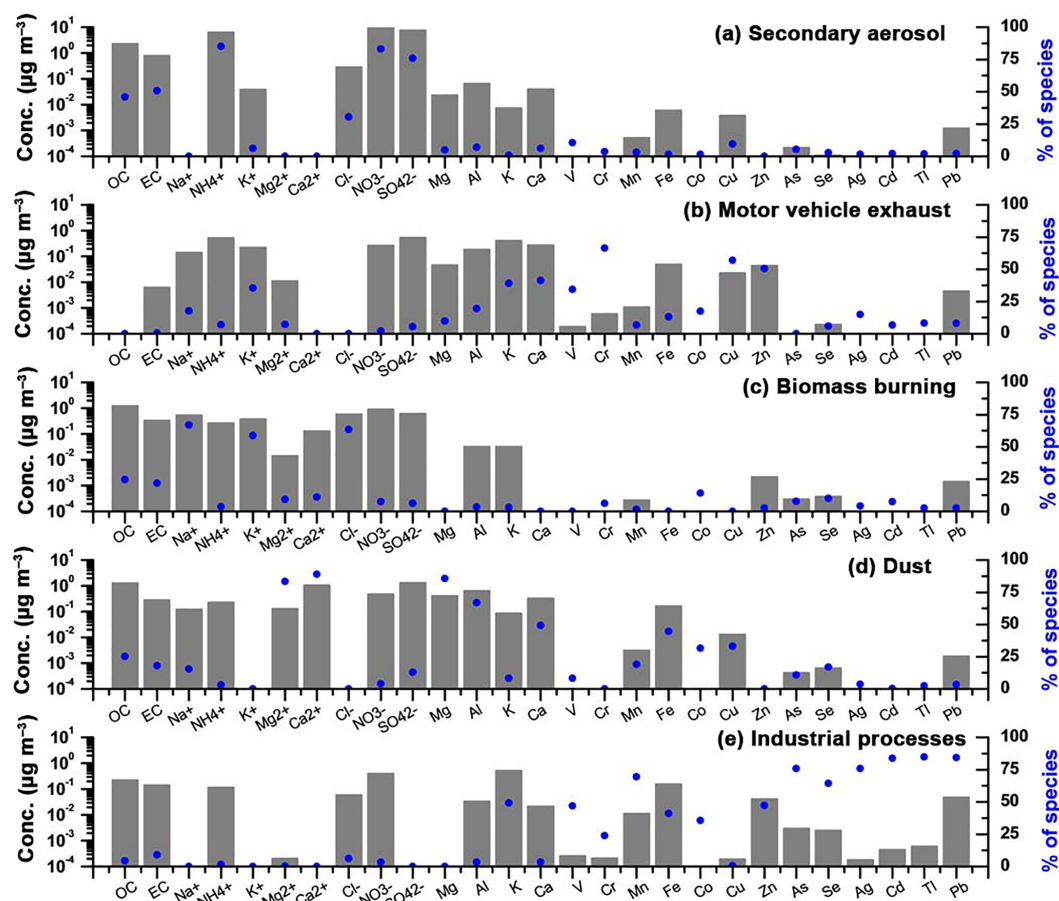
Figure 5. PMF source factor profiles for the PM$_{2.5}$ samples throughout the entire study period in Xinglong in terms of concentrations (µg m^{-3}) and percentages (%).

the coal combustion source was included in the secondary aerosol source. However, our analysis indicates that there were only very minor local coal combustion emissions in Xinglong. Therefore, this contribution can probably be attributed to the regional transport of coal combustion emissions along with secondary sources.

In Tianjin, high contributions of sulfate, nitrate, and ammonium, which comprise most of the aerosol mass concentrations, were apportioned in the secondary aerosol (Fig. S3b) with only minor OC masses; thus, we identified this factor as secondary inorganic aerosol. In contrast, in Beijing and Shijiazhuang, secondary inorganic aerosol was further separated into two sources. These are defined as nitrate-rich secondary (Figs. S2b and S4b) and sulfate-rich secondary aerosol (Figs. S2c and S4c), which record the respective characteristics of the prominent contributions of ammonium nitrate and ammonium sulfate. Consistent with the generating mechanisms and seasonal characteristics of nitrate and sulfate, the contribution of nitrate-rich secondary aerosol to PM$_{2.5}$ had the highest values in autumn,

whereas the sulfate-rich secondary aerosol had the highest contribution values in summer in Beijing and Shijiazhuang.

Motor vehicle exhaust. Emissions from motor vehicles are major factors in serious air pollution, especially in economically developed megacities. In our study, the factor of motor vehicle exhaust, which has high concentrations of OC, EC, and the trace metals Cu, Zn, and Pb that are considered to be characteristic species of dust from brake and tire wear (Gao et al., 2014; Karnae and John, 2011; Tian et al., 2016; Zhang et al., 2013), was identified at all four study sites, contributing 24.9 % (Beijing), 15.2 % (Tianjin), and 17.3 % (Shijiazhuang) of the aerosols at the urban sites and only 4.2 % in Xinglong. This suggests the important role of motor vehicle exhaust in urban PM$_{2.5}$ pollution, especially in Beijing where the number of motor vehicles increased to 5.7 million by 2016. Notably, secondary aerosols are mainly produced by the gas-to-particle transformations of SO$_2$, NO$_x$, NH$_3$, and VOCs, and motor vehicle exhaust is an important source of emissions of NO$_x$ and

VOCs in urban areas (Huang et al., 2011; Tang et al., 2016b). Therefore, the actual contribution of motor vehicle exhaust to aerosols should be higher when considering the secondary formation of gaseous exhaust in the atmosphere.

Since 2017, the vehicular emission standard of China in Phase V (equivalent to European V) has been implemented on a national scale and has caught up with developed countries. However, the less restrictive standards for oil quality in China than those in Europe and the United States are the main reason for the strong motor vehicle emissions, particularly the limits on aromatics and alkenes. These two unsaturated hydrocarbon species have important effects on air quality (Schell et al., 2001), as decreasing alkene content can decrease fire temperatures and reduce NO$_x$ emissions (G. Q. Tang et al., 2015). A new study has also reported that gasoline aromatic hydrocarbons had an essential role in urban SOA production enhancement and thus significantly affected the ambient PM$_{2.5}$ (Peng et al., 2017). The limits on aromatic and alkene contents in vehicle gasoline are respectively 40 and 28 % for China IV starting in 2014, 40 and 24 % for China V starting in 2017, and 35 and 18 % for China VI, which is suggested for implementation in 2019 (http://www.nea.gov.cn/). In contrast, the limit standards of 35 % for aromatics and 18 % for alkenes (European IV) in Europe were implemented in 2005. In addition to the lower standards for oil quality, the phenomenon of substandard oil products is also an issue. G. Q. Tang et al. (2015) reported that 48.4 % of the gasoline samples in northern China exceeded the aromatics limit (40 %).

Biomass burning. Biomass burning emissions in northern China are mainly produced by the burning of agricultural straw and thus often appear during the farming and harvest seasons. These emissions can have a significant impact on atmospheric chemistry and the climate on both a regional and global scale (Duan et al., 2004; Li et al., 2010; Sun et al., 2016). The source profiles of the factors defined as biomass burning (Figs. 5c, S2e, S3d, and S4e) were aerosols rich in K$^+$, which is widely regarded to be a good tracer of biomass burning sources. In addition to K$^+$, the fresh smoke plumes of burning biomass also contain significant amounts of Na$^+$, Cl$^-$, OC, and EC (G. H. Wang et al., 2013), which were also found in the profiles of biomass burning in this study. The annual average contribution of biomass burning to PM$_{2.5}$ showed higher values in Xinglong (8.9 %) than it did at the three urban sites (2.8–5.3 %). In addition to the high proportion during the harvest season (autumn, 11.6 %), biomass burning emissions exhibited their highest contributions to PM$_{2.5}$ in winter in Xinglong (14.6 %) and recorded low values (1.0–4.4 %) in winter at the three urban sites. This pattern can likely be attributed to the fact that a single type of fuel is used by the surrounding rural residents, as biofuels (i.e., straw and dry wood) are always utilized for cooking and winter heating (Zhao et al., 2012), which is totally different than the fuel used for energy (mainly coal and natural gas) by urban and suburban residents. Similar to the motor vehicle source, the contribution of biomass burning would be higher if the emissions of secondary aerosol precursors (VOCs, SO$_2$, and NO$_x$), especially VOCs, are considered (Bo et al., 2008; Li et al., 2014; Yuan et al., 2010).

Dust. Road dust from local traffic and construction activities (with abundant concentrations of Mg^{2+}, Ca^{2+}, and motor-vehicle-related species such as Cu, Zn, and Pb; Han et al., 2007) and soil dust, which is mainly derived from long-range transport (and is more enriched in Al, Ca, Fe, Mg, and Mn), were summarized as dust. This source was found to have an obvious seasonality, exhibiting its highest contributions in spring at the urban (17.2–21.0 %) and background sites (22.2 %). Influenced by the dust from the northwest, this seasonal variation was most significant and regular for soil dust. The factor of road dust was identified at three urban sites, which contributed annual average values of 3.5–7.8 % to PM$_{2.5}$ but was not extracted from the dust source in Xinglong due to the minor influence of anthropogenic sources.

Industrial processes. A striking feature of this source was its relatively high concentrations of mining-related elements, such as V, Mn, and Fe, and elements related to pollution produced by industrial processes, including As, Se, Ag, Cd, Tl, and Pb. More than 50 % of the mass concentrations of the above pollution elements were allocated to this source. The annual average emissions from industrial processes contributed 3.2–11.7 % to PM$_{2.5}$ at the urban sites, which was lowest in Beijing. The industrial processes source in Xinglong (2.9 %) may have been the result of regional transport from cities with heavy industrial activity. In Tianjin and Shijiazhuang (two heavily industrial cities), an oil refining and metal smelting source, characterized by high concentrations of V, Mn, Fe, Co, and Ni (Mohiuddin et al., 2014), was extracted from the emission source of industrial processes, contributing 2.8 (Tianjin) and 0.7 % (Shijiazhuang) to the PM$_{2.5}$.

In summary, secondary inorganic aerosol (40.5 %) and motor vehicle exhaust (24.9 %) were the largest PM$_{2.5}$ sources in Beijing and have greater values than the results of the 2010 study by Wu et al. (2014). The contribution of motor vehicle exhaust was close to that provided by the Beijing Municipal Environmental Protection Bureau (19.9–22.4 %; http://www.bjepb.gov.cn/; Table S3). Compared with those of Beijing, there were more complicated sources of PM$_{2.5}$ in
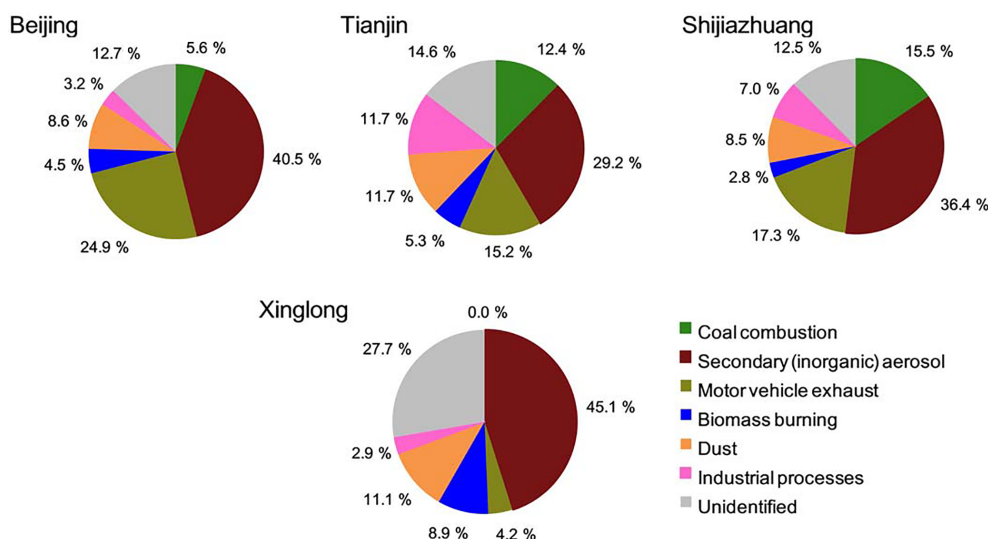
Figure 6. The annual contributions of the identified sources to PM$_{2.5}$ masses at the four sites.

Tianjin and Shijiazhuang. Motor vehicle exhaust was also an important source at the two sites, but the contribution (15.2 in Tianjin and 17.3 % in Shijiazhuang) was lower than that in Beijing, which was consistent with the results published by the Environmental Protection Bureau (EPB; Table S3). However, coal combustion became an important source in Tianjin (12.4 %) and Shijiazhuang (15.5 %), which was slightly lower than that from the Environmental Protection Bureau and that given by B. Liu et al. (2017; 16.5 % in Tianjin). The biggest PM$_{2.5}$ source in Tianjin (29.2 %) and Shijiazhuang (36.4 %) was still secondary inorganic aerosol, of which the contribution in Tianjin was close to that of B. Liu et al. (2017; 26.1 %).

3.4 Evolution at different pollution levels

By using the PM$_{2.5}$ pollution grading standards of the Air Quality Index (AQI) technical regulations (HJ 633-2012) formulated by the Chinese Ministry of Environmental Protection as a reference and considering the quantity of samples analyzed in this study, days with average concentrations of PM$_{2.5} < 75$, $75 \leq$ PM$_{2.5} < 150$, and PM$_{2.5} \geq 150 \, \mu\text{g m}^{-3}$ were defined as clean, moderate pollution, and heavy pollution days, respectively. The seasonal distributions of sample quantities at different pollution levels are listed in Table S1.

3.4.1 Evolution of chemical components

The evolution of the chemical compositions at different pollution levels during the entire observational period and in each season are shown respectively in Figs. 7 and S5, both of which show that nearly all of the chemical components increased continuously and noticeably with the aggravation of pollution. A remarkable increase in carbonaceous aerosols was observed during the pollution process, in which the an-

nual average OC and EC concentrations on heavy pollution days were 3.5–7.0 and 4.6–5.9 times as high as they were on clean days, respectively. On annual average, the OC / EC mass ratio decreased significantly with the pollution levels in Beijing, with its value varying from 3.4 (clean days), to 2.9 (moderate pollution days), to 2.1 (heavy pollution days). Tianjin also recorded a similar but milder pattern (varying from 2.3, to 2.0, to 1.9, respectively). This trend at the two sites has also been found in the investigation of specific pollution processes in summer from 29 June to 8 July, in winter from 11 to 16 January, and in spring from 23 March to 1 April (the extreme haze episode in autumn from 5 to 11 October was not analyzed due to many missing samples; Fig. 8). As reported by Watson et al. (2001), lower OC / EC ratios are emitted from motor vehicles (1.1) than from coal combustion (2.7) and biomass burning (9.0). Saarikoski et al. (2008) have also documented an OC / EC ratio of 6.6 for biomass burning and 0.71 for traffic emissions. Therefore, we speculate that this pattern of variations in the OC / EC ratio in Beijing may be influenced by the strengthened contributions of local motor vehicle exhaust under heavily polluted conditions due to weakened regional transport, which usually contributes most during the initial and growth stages of haze episodes but decreases during the peak pollution stage. This mechanism has been confirmed in some specific pollution processes in Beijing (Z. R. Liu et al., 2016; G. Tang et al., 2015). By using CAMx (Comprehensive Air Quality Model with Extensions), Wang et al. (2017) also documented that the extreme haze episode during January 2013 in urban Beijing was dominated by local contributions. Therefore, the fact that the OC / EC ratio decreases with the increasing development of haze pollution indicates the key role of local traffic emissions in the haze processes of Beijing.
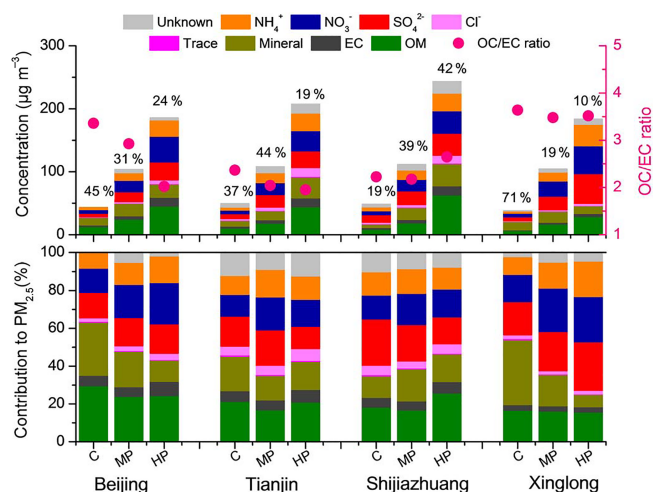
Figure 7. The evolution of aerosol chemical species and the OC / EC mass ratio (marked with pink dots) at different pollution levels during the entire observational period. C, MP, and HP represent clean days (PM$_{2.5} < 75\,\mu g\,m^{-3}$), moderate pollution days ($75 \leq$ PM$_{2.5} < 150\,\mu g\,m^{-3}$), and heavy pollution days (PM$_{2.5} \geq 150\,\mu g\,m^{-3}$), respectively; "%" represents the proportion of the filter sample quantity at each pollution level out of the total samples.

In addition, SNA generally significantly contribute to the enhancement of the PM$_{2.5}$ mass during pollution events, particularly in Beijing and Xinglong as the contribution of SNA increased remarkably from 34.5 % on clean days, to 44.2 % on moderate pollution days, to 51.3 % on heavy pollution days in Beijing and from 41.2, to 57.5, to 68.3 %, respectively, in Xinglong (Fig. 7). Sulfate, nitrate, and ammonium all clearly increased with the aggravation of pollution in Xinglong, suggesting that its high PM$_{2.5}$ loadings mainly resulted from the intensifying secondary transformation of gaseous pollutants (SO$_2$, NO$_x$, and NH$_3$) during stagnant meteorological conditions in the background area. However, in Beijing, only the contribution of nitrate (except in summer), the formation of which is locally dominant (Guo et al., 2010), experienced a pronounced increase during the pollution process (Fig. S5). This indicates that the haze pollution in Beijing mainly resulted from the secondary transformation of NO$_x$ that was mainly derived from local traffic emissions, once again reflecting the dominant contribution of local motor vehicle exhaust to Beijing haze episodes. An average increase in the contributions of SNA during the pollution process was not observed but did occur in all seasons except for spring in Tianjin and Shijiazhuang (Fig. S5), while the mineral dust contribution increased considerably in spring, indicating the important role of dust in the formation of spring haze at the two study sites.

From the above analysis, it can be seen that the chemical characteristics of haze pollution varied by site and season. The most prominent feature in summer was the inten-

sive formation of SNA, which was observed simultaneously at the three urban sites on a regional scale during the period from 29 June to 8 July (Fig. 8a). The SNA contributed to the elevation of the PM$_{2.5}$ concentration. SNA showed a substantial increase by a factor of 5.7, from 22.6 $\mu g\,m^{-3}$ during the clean period to 128.7 $\mu g\,m^{-3}$ during the haze episodes (2 July-N to 4 July-N and 5 July-N to 7 July-N) in Beijing, and a corresponding increase on the contribution of SNA to PM$_{2.5}$ from 45.7 to 72.5 %; the enhancement ratios were 4.4 and 3.4 in Tianjin and Shijiazhuang, respectively. The large increase in the concentrations and contributions of SNA during the haze process was observed in many previous studies and is mainly attributed to enhanced secondary conversions via enhanced heterogeneous reactions under relatively high humidity conditions during the haze periods (Fig. S6; averaging 67 % during haze episodes and 37 % during clean periods in summer in Beijing, as measured in this study; Huang et al., 2016; Sun et al., 2013; X. F. Wang et al., 2012; Yang et al., 2015). The degree of the secondary formation of sulfate and nitrate is commonly estimated using the sulfur oxidation ratio (SOR $= n$-SO$_4^{2-}/n$-SO$_4^{2-} + n$-SO$_2$, where n refers to molar concentration) and the nitrogen oxidation ratio (NOR $= n$-NO$_3^-/n$-NO$_3^- + n$-NO$_2$), respectively (Huang et al., 2016; X. J. Zhao et al., 2013). Higher values of the SOR and NOR indicate that more gaseous SO$_2$ and NO$_2$ would be oxidized to sulfate and nitrate in the atmosphere. In this study, the SOR and NOR were significantly elevated during the increases in PM$_{2.5}$ concentrations in the summer period and remained at a high level during haze episodes in Beijing (averaging 0.92 for SOR and 0.38 for NOR), Tianjin (0.83 and 0.41), and Shijiazhuang (0.65 and 0.44). In autumn, Yang et al. (2015) also revealed that the intense secondary formation of SNA contributed most to the formation of the hazes in October 2014, with the SOR and NOR values increasing considerably during the haze episodes. Similar variations were also observed in winter, but the formation of SNA in winter was much weaker than that in summer and autumn, with SOR values of only 0.18–0.35 and NOR values of 0.20–0.22 during the regional haze episode (13 to 15 January) at the three urban sites. However, the increases in the SNA concentrations were still significant during this haze episode. In addition, the increase in OM was pronounced during the winter regional haze episode, exhibiting the highest OM values during this episode with average values of 57.3, 51.8, and 133.4 $\mu g\,m^{-3}$ in Beijing, Tianjin, and Shijiazhuang, respectively, which were 3.5, 4.1, and 5.9 times those during the clean periods, while the enhancement ratio was only 1.1–1.4 in the summer period. Therefore, SNA and OM both increased substantially and dominated the PM$_{2.5}$ during the winter haze episode, such that the respective contributions of SNA and OM were 42.6 and 26.1 % in Beijing, 53.8 and 23.3 % in Tianjin, and 43.2 and 37.0 % in Shijiazhuang. The phenomenon of the significant increase in SNA and OM in the winter haze episode was also observed by Zhao et al. (2013c) and Huang et al. (2014), indicating that the winter
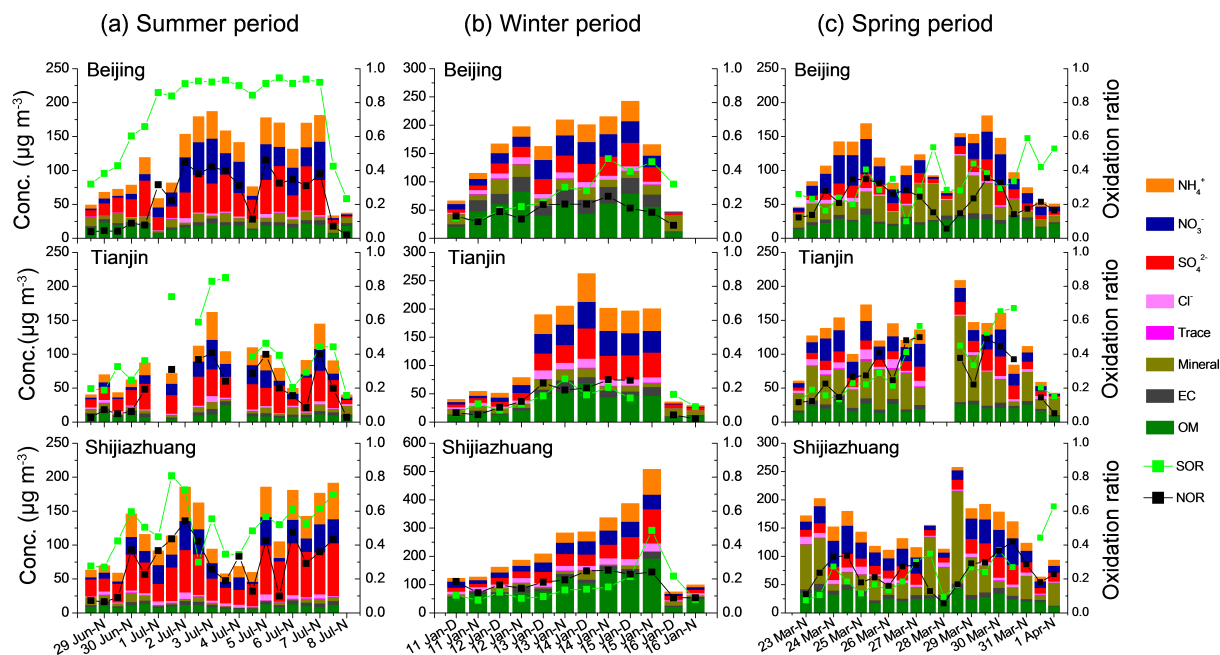
Figure 8. The evolution of the chemical species, sulfur oxidation rate (SOR), and nitrogen oxidation rate (NOR) in the specific pollution periods in summer **(a)**, winter **(b)**, and spring **(c)** at the urban sites. D: daytime; N: nighttime.
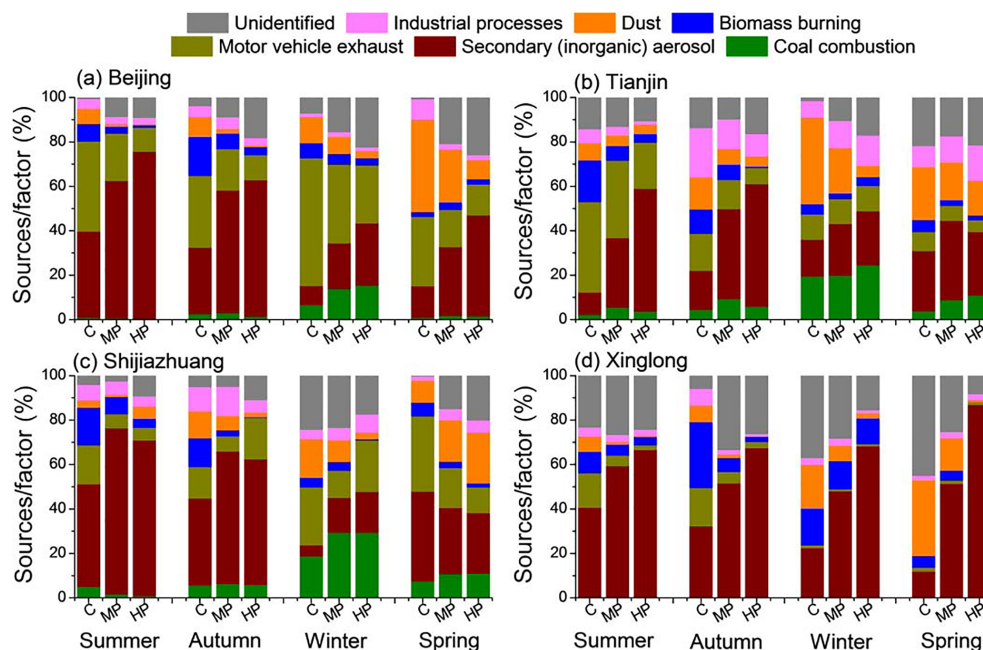

Figure 9. Fractional contributions of source factors to the PM$_{2.5}$ masses at different pollution levels during each season in Beijing **(a)**, Tianjin **(b)**, Shijiazhuang **(c)**, and Xinglong **(d)**. C, MP, and HP represent clean days (PM$_{2.5}$ < 75 µg m^{-3}), moderate pollution days (75 ≤ PM$_{2.5}$ < 150 µg m^{-3}), and heavy pollution days (PM$_{2.5}$ ≥ 150 µg m^{-3}), respectively.

haze may be largely driven by secondary aerosol formation, which could be identified as a common characteristic of winter pollution in this region. Compared to winter, the SOR and NOR values increased on the whole in spring, but their variations, and the variations in SNA and OM, had no apparent

regular connection with the fluctuation of PM$_{2.5}$, especially in Tianjin and Shijiazhuang. In contrast to observations in summer and winter, the most striking feature of spring pollution was the enhanced contribution of mineral dust; during the regional dust–haze episode from 29 March-D to 30-N,

the contribution of the mineral dust even reached 60.3 % in Shijiazhuang, 51.7 % in Tianjin, and 47.8 % in Beijing on 29 March-D under the conditions of a strong northerly wind (Fig. S6). Subsequently, mineral dust decreased, while SNA rose gradually with the increase in relative humidity and the shift of the wind direction (Figs. 8 and S6). The contribution of SNA to PM$_{2.5}$ rose to 61.3, 53.9, and 55.0 % on 30 March-N in Beijing, Tianjin, and Shijiazhuang, respectively, again exhibiting secondary pollution characteristics.

3.4.2 Evolution of source contributions

In addition to the evolution of the chemical components during the transitions from clean to pollution processes, significant variations in the contributions of sources were also observed and exhibited strong seasonal features and spatial heterogeneities (Fig. 9). However, the common characteristic of each season and site was that the secondary aerosol and inorganic aerosol played a key role in the development of haze pollution, with generally increasing contributions with worsening pollution (except in spring of Shijiazhuang), which was also reported by Huang et al. (2014). Especially in summer and autumn, secondary inorganic aerosol increased most dramatically as a function of high relative humidity and suitable temperature at the urban sites; on heavy pollution days, it accounted for 55.7–75.2 % of the PM$_{2.5}$ in summer and 55.0–61.5 % in autumn, thus representing the biggest source of atmospheric PM$_{2.5}$ during these two seasons. In contrast, in Xinglong, the secondary aerosol source was always the dominant factor in haze formation, which accounted for 66.7, 67.5, 68.4, and 87.0 % of the PM$_{2.5}$ on heavy pollution days in summer, autumn, winter, and spring, respectively. In addition, biomass burning was another important source during the winter pollution process in Xinglong.

In contrast to the background site, the emission sources and generation mechanisms of haze pollution were more complex at the urban sites, especially in winter, as the primary emissions, such as motor vehicle exhaust, coal combustion, and industrial processes, were also the main sources of heavy pollution in winter. As the main fuel for winter heating in northern China, coal combustion was crucial to the heavy pollution in winter in urban areas, as its contribution increases with increasing pollution levels. In Tianjin and Shijiazhuang, this source contributed nearly 30 % to the PM$_{2.5}$ on heavy pollution days and contributed even more when considering the secondary formation of gaseous precursors emitted by coal combustion. Moreover, the primary emissions of motor vehicles also exerted a remarkable impact on the winter haze pollution, accounting for 26.1 % of PM$_{2.5}$ on heavy pollution days in Beijing and accounting for more when the secondary conversion of gaseous pollutants in vehicle exhaust is considered, as nitrate-rich secondary aerosol increased from 2.9 % on clean days to 19.5 % on heavy pollution days during the winter period. On hazy days, low visibility could aggravate urban traffic congestion during rush hour,

thus causing more pollutants to be emitted by motor vehicles operating in these conditions (Zhang et al., 2011). Therefore, the winter haze was mainly formed by local processes (local direct emissions and secondary transformation).

In spring, the effect of a dust source was highlighted at the urban sites. Most notably in Shijiazhuang, the mineral dust source significantly contributed to the aerosol pollution process, as its contribution to PM$_{2.5}$ continuously increased from 9.7 % on clean days, to 18.6 % on moderate pollution days, to 22.9 % on heavy pollution days. However, along with the increase in pollution levels, the ratio of the local road dust source to the overall dust source decreased from 81.6 (on clean days) to 50 % (on pollution days), thus reflecting the significant impact of the long-range transport of northwest dust on the spring aerosol pollution in Shijiazhuang. Differing from the increase in relative humidity during haze episodes in the other seasons, the relative humidity decreased continuously from 64 (clean days), to 47 % (moderate pollution days), to 40 (heavy pollution days) in spring in Shijiazhuang (Table S2). Therefore, the heterogeneous reactions promoted by enhanced water vapor may not be the spring haze formation mechanism in Shijiazhuang, as the contribution of secondary inorganic aerosol decreased remarkably during the haze episode (Figs. 9 and S5). In contrast, the wind speed and the contribution of the dust source significantly increased during the spring haze period in Shijiazhuang. A similar but much milder pattern (except in terms of wind speed) was also recorded in Tianjin. Therefore, dust pollution, which was mainly the result of long-range transported soil dust and local road dust, contributed to the spring haze in Shijiazhuang and Tianjin.

3.5 Backward-trajectory analysis

To reveal the pollution patterns and source signals of the PM$_{2.5}$ carried by air masses from different directions and regions, the source contributions of PM$_{2.5}$ were grouped according to their trajectory clusters, as shown in Fig. 10. The results in Fig. 10 indicate the important effects of regional transport on PM$_{2.5}$. More than half of the air masses (54, 64, 51, and 56 % for Beijing, Tianjin, Shijiazhuang, and Xinglong, respectively) in the entire study period were from the BTH region and Shandong Province. These air masses, which move at slow speeds and at low heights, could have carried abundant atmospheric pollutants (i.e., particles and gaseous pollutants) from the areas through which they passed, which may have been accompanied by plenty of water vapor during the transport process (Tao et al., 2012; Zhu et al., 2016), resulting in high PM$_{2.5}$ mass concentrations driven by local secondary formation at the sampling sites. The air masses (cluster 1 at each site) from the southern direction caused the most serious pollution. Air masses originating from Mongolia were also dominant (27–46 %) in this region (clusters 2–3 in Beijing, clusters 4–5 at Tianjin, clusters 3–4 at Shijiazhuang, and cluster 3 in Xinglong), and the
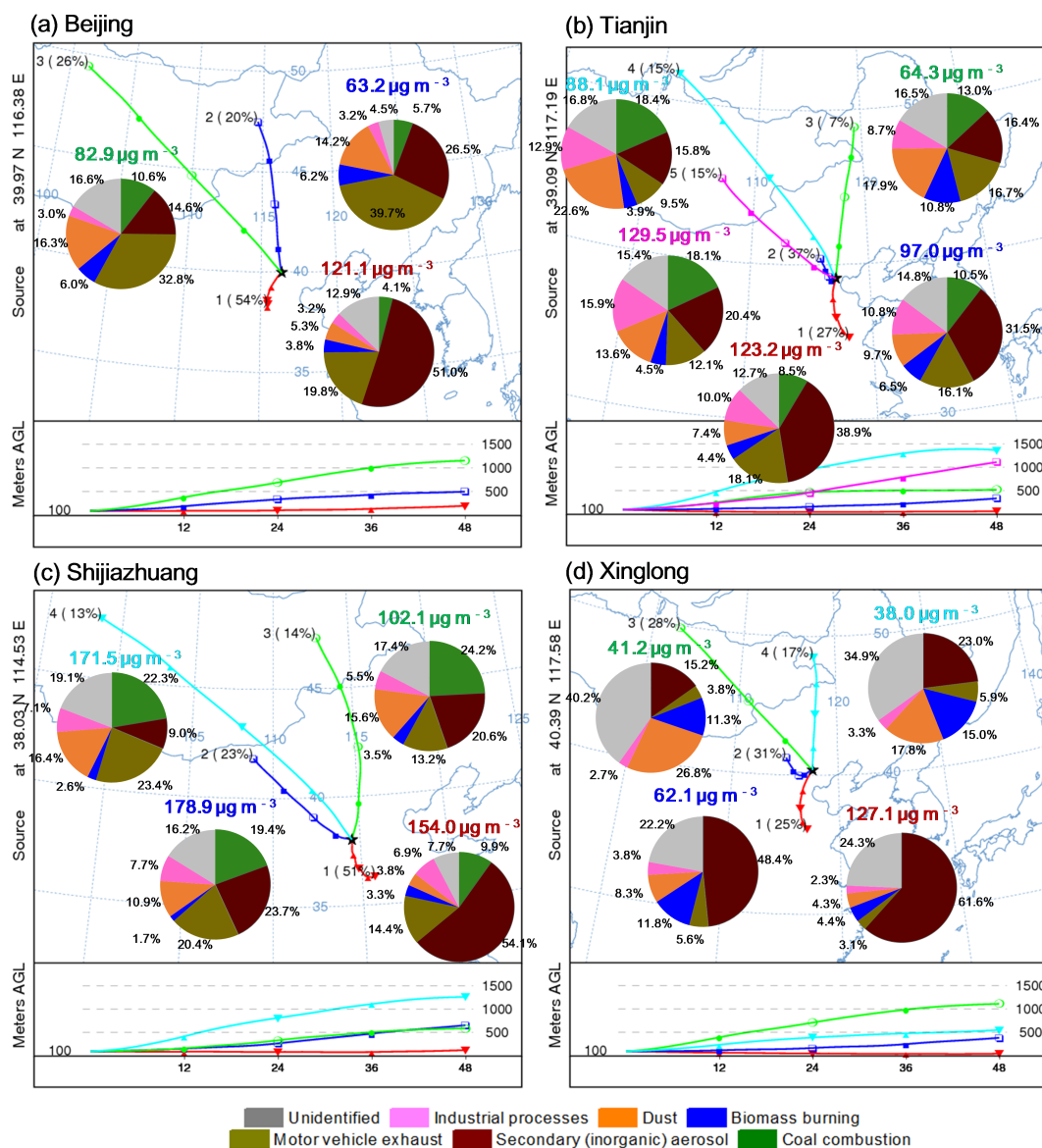
Figure 10. Source contributions resolved from the PMF at each 48 h backward-trajectory cluster during the entire study period in Beijing **(a)**, Tianjin **(b)**, Shijiazhuang **(c)**, and Xinglong **(d)**.

PM$_{2.5}$ in these clusters was generally lower than in the surrounding polluted areas, except for Shijiazhuang and Tianjin in cluster 5 (Fig. 10b). In addition, a small proportion of air masses originating from the Hulunbuir prairie in Inner Mongolia, such as those in cluster 3 in Tianjin and in cluster 4 in Xinglong, could have carried clean air to the sampling sites, thus causing the corresponding PM$_{2.5}$ mass concentrations to be the lowest. In contrast to the other sites, the highest average PM$_{2.5}$ concentrations of each cluster were observed in Shijiazhuang, especially in cluster 2, which originated from Inner Mongolia and passed over Shanxi Province before arriving at the sampling sites and corresponded to the highest PM$_{2.5}$ value (178.9 μg m^{-3}). Although cluster 4 originated

from Mongolia and traveled at fast speeds and higher heights, the PM$_{2.5}$ was indeed higher than that of cluster 1, which may be because it passed over Inner Mongolia and Shanxi Province and thus could have carried many pollutants from these polluted areas. The PM$_{2.5}$ concentration in cluster 3, which originated from Mongolia and passed over Inner Mongolia and northern Hebei (a relatively clean area in the BTH region), was relatively lower (102.1 μg m^{-3}). However, the heavy pollution in Shijiazhuang was mainly dominated by cluster 1 (51 %) from the south, as cluster 2 and cluster 4 accounted for only 23 and 13 % of the trajectories, respectively. Similarly, the haze pollution in Beijing, Tianjin, and Xinglong also developed due to the presence of weak southerly

air masses from heavily polluted regions. This is consistent with the results of Guo et al. (2014) and Li et al. (2015).

In addition to the different PM$_{2.5}$ concentrations in the different clusters, considerable differences in the source contributions were also found. For example, in Shijiazhuang, high PM$_{2.5}$ concentrations were observed in each cluster. However, it could also be clearly seen that the source contribution charts of these clusters were very different and that the air masses originating from the BTH region and Shandong Province were characterized by a high contribution from secondary inorganic aerosol, while the air masses from long-range transport were more enriched in dust. Therefore, in Shijiazhuang, the contribution of secondary inorganic aerosol occurred such that cluster 1 > cluster 2 > cluster 3 > cluster 4, whereas that of the dust source exhibited the opposite pattern. Similar patterns were also observed for Xinglong, Beijing, and Tianjin in this study. This pattern of secondary inorganic aerosol was also observed by Zhang et al. (2014) in their study in Beijing. As mentioned in Sect. 3.3, secondary aerosol was primarily attributed to the transformation of precursors (SO$_2$, NO$_x$, NH$_3$, and VOCs). The slow and near-ground air masses originating from the regional polluted areas could have resulted in stagnant conditions, which could have been conducive to the accumulation of precursors from local emissions and those transported in and to the following secondary transformation. Furthermore, during this transportation, the carried gaseous pollutants could also have undergone secondary transformations and directly resulted in rapid increases in PM$_{2.5}$ concentrations in the downwind area (Bressi et al., 2014; Li et al., 2015). Our previous study also revealed that the high concentrations of organic aerosols (OAs) in Beijing, especially low-volatility oxygenated aerosols that are more oxidized and aged, were associated with south-originating air masses containing secondary regional pollutants (J. K. Zhang et al., 2015).

4   Conclusions

In this study, the chemical compositions and emission sources of fine particulate matter (PM$_{2.5}$) were comprehensively investigated at three urban sites (Beijing, Tianjin, and Shijiazhuang) and a background site (Xinglong) in the BTH region. Severe PM$_{2.5}$ pollution was found at all three urban sites, especially in Shijiazhuang, and the background site was found to be relatively clean. The seasonal variations in the PM$_{2.5}$ concentrations in Xinglong were not significant due to the presence of fewer anthropogenic emissions. At the urban sites, the lowest PM$_{2.5}$ values were observed in summer and the highest values were observed in winter, likely due to the prevalence of winter coal-fired heating and unfavorable meteorological conditions. The chemical compositions of PM$_{2.5}$ were similar at the four sites, and the major chemical components were organic matter, secondary inorganic ions (sulfate, nitrate, ammonium), and mineral dust. These components showed distinctive seasonal variability, which was closely related to chemical processes, emission sources, and meteorological conditions. Organic matter and elemental carbon had the highest recorded values and contributions to PM$_{2.5}$ in winter and sulfate peaked in summer, while nitrate peaked in autumn and mineral dust peaked in spring.

The PMF model-resolved source analysis showed that coal combustion, motor vehicle exhaust, secondary inorganic aerosol, dust, and industrial processes were the main sources of PM$_{2.5}$ in urban areas; however, the dominant source at the background site was secondary aerosol. The drastic secondary transformation of gas precursors was the dominant cause of aerosol pollution, especially in summer and autumn. In winter, local direct emissions (coal combustion and motor vehicle exhaust) and secondary formation greatly impacted haze formation in urban areas. In spring, the dust source exerted a significant impact and dominated the pollution in Shijiazhuang and Tianjin. In urban atmospheres, especially in Beijing, the contribution of motor vehicle exhaust was also prominent in haze formation, as it is the major source of gaseous NO$_x$. However, in this study, we could not determine the exact contribution of the secondary transformation of the NO$_x$ emitted by motor vehicles. Future studies should investigate additional details about these secondary aerosols.

Haze pollution has remarkable regional characteristics, and the severe pollution in the BTH region was mainly influenced by the region itself and its surrounding polluted areas to the south. Therefore, we question the efficiency of the abatement strategies for emission reduction and air quality improvement and suggest a joint collaboration of cities in this region, perhaps even throughout all of northern China. The reduction of gaseous precursors from fossil fuel combustion, which equates to the reduction of emissions from motor vehicles in Beijing by improving oil quality, and those from coal combustion from Tianjin, Hebei, and the surrounding heavily polluted provinces is essential to mitigate the severe haze pollution in the BTH region.

The Supplement related to this article is available online at https://doi.org/10.5194/acp-17-12941-2017-supplement.

References

Arimoto, R., Duce, R. A., Savoie, D. L., Prospero, J. M., Talbot, R., Cullen, J. D., Tomza, U., Lewis, N. F., and Ray, B. J.: Relationships among aerosol constituents from Asia and the North Pacific during PEM-West A, J. Geophys. Res.-Atmos., 101, 2011–2023, https://doi.org/10.1029/95JD01071, 1996.

Bo, Y., Cai, H., and Xie, S. D.: Spatial and temporal variation of historical anthropogenic NMVOCs emission inventories in China, Atmos. Chem. Phys., 8, 7297–7316, https://doi.org/10.5194/acp-8-7297-2008, 2008.

Bressi, M., Sciare, J., Ghersi, V., Bonnaire, N., Nicolas, J. B., Petit, J. E., Moukhtar, S., Rosso, A., Mihalopoulos, N., and Féron, A.: A one-year comprehensive chemical characterisation of fine aerosol (PM2.5) at urban, suburban and rural background sites in the region of Paris (France), Atmos. Chem. Phys., 13, 7825–7844, https://doi.org/10.5194/acp-13-7825-2013, 2013.

Bressi, M., Sciare, J., Ghersi, V., Mihalopoulos, N., Petit, J. E., Nicolas, J. B., Moukhtar, S., Rosso, A., Féron, A., Bonnaire, N., Poulakis, E., and Theodosi, C.: Sources and geographical origins of fine aerosols in Paris (France), Atmos. Chem. Phys., 14, 8813–8839, https://doi.org/10.5194/acp-14-8813-2014, 2014.

Cai, W., Li, K., Liao, H., Wang, H., and Wu, L.: Weather conditions conducive to Beijing severe haze more frequent under climate change, Nat. Clim. Chang. Press, March, https://doi.org/10.1038/NCLIMATE3249, 2017.

Cao, J. J., Lee, S. C., Ho, K. F., Zou, S. C., Fung, K., Li, Y., Watson, J. G., and Chow, J. C.: Spatial and seasonal variations of atmospheric organic carbon and elemental carbon in Pearl River Delta Region, China, Atmos. Environ., 38, 4447–4456, https://doi.org/10.1016/j.atmosenv.2004.05.016, 2004.

Cao, J. J., Lee, S. C., Chow, J. C., Watson, J. G., Ho, K. F., Zhang, R. J., Jin, Z. D., Shen, Z. X., Chen, G. C., Kang, Y. M., Zou, S. C., Zhang, L. Z., Qi, S. H., Dai, M. H., Cheng, Y., and Hu, K.: Spatial and seasonal distributions of carbona-ceous aerosols over China, J. Geophys. Res., 112, D22S11, https://doi.org/10.1029/2006jd008205, 2007.

Cao, J. J., Shen, Z. X., Chow, J. C., Qi, G. W., and Watson, J. G.: Seasonal variations and sources of mass and chemical composition for PM10 aerosol in Hangzhou, China, Particuology, 7, 161–168, https://doi.org/10.1016/j.partic.2009.01.009, 2009.

Chen, D., Liu, X., Lang, J., Zhou, Y., Wei, L., Wang, X., and Guo, X.: Estimating the contribution of regional transport to PM2.5 air pollution in a rural area on the North China Plain, Sci. Total Environ., 583, 280–291, https://doi.org/10.1016/j.scitotenv.2017.01.066, 2017.

Cheng, Y. F., Zheng, G. J., Wei, C., Mu, Q., Zheng, B., Wang, Z. B., Gao, M., Zhang, Q., He, K. B., Carmichael, G., Pöschl, U., and Su, H.: Reactive nitrogen chemistry in aerosol water as a source of sulfate during haze events in China, Sci. Adv., 2, e1601530, https://doi.org/10.1126/sciadv.1601530, 2016.

Christoforou, C. S., Salmon, L. G., Hannigan, M. P., Solomon, P. A., and Cass, G. R.: Trends in Fine Particle Concentration and Chemical Composition in Southern California, J. Air Waste Manage. Assoc., 50, 43–53, https://doi.org/10.1080/10473289.2000.10463985, 2000.

Du, Z., He, K., Cheng, Y., Duan, F., Ma, Y., Liu, J., Zhang, X., Zheng, M., and Weber, R.: A yearlong study of water-soluble organic carbon in Beijing I: Sources and its primary vs. secondary nature, Atmos. Environ., 92, 514–521, https://doi.org/10.1016/j.atmosenv.2014.04.060, 2014.

Duan, F., Liu, X., Yu, T., and Cachier, H.: Identification and estimate of biomass burning contribution to the urban aerosol organic carbon concentrations in Beijing, Atmos. Environ., 38, 1275–1282, https://doi.org/10.1016/j.atmosenv.2003.11.037, 2004.

Elliot, A. J., Smith, S., Dobney, A., Thornes, J., Smith, G. E., and Vardoulakis, S.: Monitoring the effect of air pollution episodes on health care consultations and ambulance call-outs in England during March/April 2014: A retrospective observational analysis, Environ. Pollut., 214, 903–911, https://doi.org/10.1016/j.envpol.2016.04.026, 2016.

Gao, J., Tian, H., Cheng, K., Lu, L., Wang, Y., Wu, Y., Zhu, C., Liu, K., Zhou, J., Liu, X., Chen, J., and Hao, J.: Seasonal and spatial variation of trace elements in multi-size airborne particulate matters of Beijing, China: Mass concentration, enrichment characteristics, source apportionment, chemical speciation and bioavailability, Atmos. Environ., 99, 257–265, https://doi.org/10.1016/j.atmosenv.2014.08.081, 2014.

Gao, J., Tian, H., Cheng, K., Lu, L., Zheng, M., Wang, S., Hao, J., Wang, K., Hua, S., Zhu, C., and Wang, Y.: The variation of chemical characteristics of PM2.5 and PM10 and formation causes during two haze pollution events in urban Beijing, China, Atmos. Environ., 107, 1–8, https://doi.org/10.1016/j.atmosenv.2015.02.022, 2015.

Gu, J., Bai, Z., Li, W., Wu, L., Liu, A., Dong, H., and Xie, Y.: Chemical composition of PM2.5 during winter in Tianjin, China, Particuology, 9, 215–221, https://doi.org/10.1016/j.partic.2011.03.001, 2011.

Guo, S., Hu, M., Wang, Z. B., Slanina, J., and Zhao, Y. L.: Size-resolved aerosol water-soluble ionic compositions in the summer of Beijing: implication of regional secondary formation, Atmos. Chem. Phys., 10, 947–959, https://doi.org/10.5194/acp-10-947-2010, 2010.

Guo, S., Hu, M., Zamora, M. L., Peng, J., Shang, D., Zheng, J., Du, Z., Wu, Z., Shao, M., Zeng, L., Molina, M. J., and Zhang, R.: Elucidating severe urban haze formation in China, P. Natl. Acad. Sci. USA, 111, 17373–17378, https://doi.org/10.1073/pnas.1419604111, 2014.

Han, B., Zhang, R., Yang, W., Bai, Z., Ma, Z., and Zhang, W.: Heavy haze episodes in Beijing during January 2013: Inorganic ion chemistry and source analysis using highly time-resolved measurements from an urban site, Sci. Total Environ., 544, 319–329, https://doi.org/10.1016/j.scitotenv.2015.10.053, 2016.

Han, L., Zhuang, G., Cheng, S., Wang, Y., and Li, J.: Characteristics of re-suspended road dust and its impact on the atmospheric environment in Beijing, Atmos. Environ., 41, 7485–7499, https://doi.org/10.1016/j.atmosenv.2007.05.044, 2007.

He, H., Wang, Y. S., Ma, Q. X., Ma, J. Z., Chu, B. W., Ji, D., Tang, G. Q., Liu, C., Zhang, H. X., and Hao, J. M.: Mineral dust and NOx promote the conversion of SO2 to sulfate in heavy pollution days, Sci. Rep., 4, 1–6, https://doi.org/10.1038/srep04172, 2014.

Hu, M., Peng, J., Sun, K., Yue, D., Guo, S., Wiedensohler, A., and Wu, Z.: Estimation of size-resolved ambient particle density based on the measurement of aerosol number, mass, and chemical size distributions in the winter in Beijing, Environ. Sci. Technol., 46, 9941–9947, https://doi.org/10.1021/es204073t, 2012.

Huang, C., Chen, C. H., Li, L., Cheng, Z., Wang, H. L., Huang, H. Y., Streets, D. G., Wang, Y. J., Zhang, G. F., and Chen, Y. R.: Emission inventory of anthropogenic air pollutants and VOC species in the Yangtze River Delta region, China, Atmos. Chem. Phys., 11, 4105–4120, https://doi.org/10.5194/acp-11-4105-2011, 2011.

Huang, K., Zhuang, G., Lin, Y., Li, J., Sun, Y., Zhang, W., and Fu, J. S.: Relation between optical and chemical properties of dust aerosol over Beijing, China, China, J. Geophys. Res, 115, 1–13, https://doi.org/10.1029/2009JD013212, 2010.

Huang, R. J., Zhang, Y., Bozzetti, C., Ho, K. F., Cao, J. J., Han, Y., Daellenbach, K. R., Slowik, J. G., Platt, S. M., Canonaco, F., Zotter, P., Wolf, R., Pieber, S. M., Bruns, E. A., Crippa, M., Ciarelli, G., Piazzalunga, A., Schwikowski, M., Abbaszade, G., Schnelle-Kreis, J., Zimmermann, R., An, Z., Szidat, S., Baltensperger, U., El Haddad, I., and Prevot, A. S.: High secondary aerosol contribution to particulate pollution during haze events in China, Nature, 514, 218–222, https://doi.org/10.1038/nature13774, 2014.

Huang, X. J., Liu, Z. R., Zhang, J. K., Wen, T. X., Ji, D. S., and Wang, Y. S.: Seasonal variation and secondary formation of size-segregated aerosol water-soluble inorganic ions during pollution episodes in Beijing, Atmos. Res., 168, 70–79, https://doi.org/10.1016/j.atmosres.2015.08.021, 2016.

Ianniello, A., Spataro, F., Esposito, G., Allegrini, I., Hu, M., and Zhu, T.: Chemical characteristics of inorganic ammonium salts in PM$_{2.5}$ in the atmosphere of Beijing (China), Atmos. Chem. Phys., 11, 10803–10822, https://doi.org/10.5194/acp-11-10803-2011, 2011.

Karnae, S. and John, K.: Source apportionment of fine particulate matter measured in an industrialized coastal urban area of South Texas, Atmos. Environ., 45, 3769–3776, https://doi.org/10.1016/j.atmosenv.2011.04.040, 2011.

Li, J., Du, H. Y., Wang, Z. F., Sun, Y. Le, Yang, W. Y., Li, J. J., Tang, X., and Fu, P. Q.: Rapid formation of a severe regional winter haze episode over a mega-city cluster on the North China Plain, Environ. Pollut., 223, 605–615, https://doi.org/10.1016/j.envpol.2017.01.063, 2017.

Li, L., Chen, Y., Zeng, L., Shao, M., Xie, S., Chen, W., Lu, S., Wu, Y., and Cao, W.: Biomass burning contribution to ambient volatile organic compounds (VOCs) in the chengdu-chongqing region (CCR), China, Atmos. Environ., 99, 403–410, https://doi.org/10.1016/j.atmosenv.2014.09.067, 2014.

Li, P. F., Yan, R. C., Yu, S. C., Wang, S., Liu, W. P., and Bao, H. M.: Reinstate regional transport of PM2.5 as a major cause of severe haze in Beijing, P. Natl. Acad. Sci. USA, 112, 2–3, https://doi.org/10.1073/pnas.1502596112, 2015.

Li, W. J., Shao, L. Y., and Buseck, P. R.: Haze types in Beijing and the influence of agricultural biomass burning, Atmos. Chem. Phys., 10, 8119–8130, https://doi.org/10.5194/acp-10-8119-2010, 2010.

Li, X. R., Song, A. L., Wang, Y. F., Sun, Y., Liu, Z. R., and Wang, Y. S.: Analysis on water-soluble inorganic ions in the atmosphereic aerosol of Xinglong, Environ. Sci., 34, 15–20, 2013 (in Chinese).

Liang, C. S., Duan, F. K., He, K. B., and Ma, Y. L.: Review on recent progress in observations, source identifications and countermeasures of PM2.5, Environ. Int., 86, 150–170, https://doi.org/10.1016/j.envint.2015.10.016, 2016.

Liu, B., Yang, J., Yuan, J., Wang, J., Dai, Q., Li, T., Bi, X., Feng, Y., Xiao, Z., Zhang, Y., and Xu, H.: Source apportionment of atmospheric pollutants based on the online data by using PMF and ME2 models at a megacity, China, Atmos. Res., 185, 22–31, https://doi.org/10.1016/j.atmosres.2016.10.023, 2017.

Liu, T. T., Gong, S. L., He, J. J., Yu, M., Wang, Q. F., Li, H. R., Liu, W., Zhang, J., Li, L., Wang, X. G., Li, S. L., Lu, Y. L., Du, H. T., Wang, Y. Q., Zhou, C. H., Liu, H. L., and Zhao, Q. C.: Attributions of meteorological and emission factors to the 2015 winter severe haze pollution episodes in China's Jing-Jin-Ji area, Atmos. Chem. Phys., 17, 2971–2980, https://doi.org/10.5194/acp-17-2971-2017, 2017.

Liu, Z. R., Hu, B., Zhang, J. K., Yu, Y. C., and Wang, Y. S.: Characteristics of aerosol size distributions and chemical compositions during wintertime pollution episodes in Beijing, Atmos. Res., 168, 1–12, https://doi.org/10.1016/j.atmosres.2015.08.013, 2016a.

Liu, Z. R., Wang, Y. S., Hu, B., Ji, D. S., Zhang, J. K., Wu, F. K., Wan, X., and Wang, Y. H.: Source appointment of fine particle number and volume concentration during severe haze pollution in Beijing in January 2013, Environ. Sci. Pollut. Res., 23, 6845–6860, https://doi.org/10.1007/s11356-015-5868-6, 2016b.

Mason, B.: Principles of Geochemistry, New York, Wiley, 1966.

Mohiuddin, K., Strezov, V., Nelson, P. F., and Stelcer, E.: Characterisation of trace metals in atmospheric particles in the vicinity of iron and steelmaking industries in Australia, Atmos. Environ., 83, 72–79, https://doi.org/10.1016/j.atmosenv.2013.11.011, 2014.

Peng, J., Hu, M., Du, Z., Wang, Y., Zheng, J., Zhang, W., Yang, Y., Qin, Y., Zheng, R., Xiao, Y., Wu, Y., Lu, S., Wu, Z., Guo, S., Mao, H., and Shuai, S.: Gasoline aromatics: a critical determinant of urban secondary organic aerosol formation, Atmos. Chem. Phys., 17, 10743–10752, https://doi.org/10.5194/acp-17-10743-2017, 2017.

Reff, A., Eberly, S. I., and Bhave, P. V.: Receptor Modeling of Ambient Particulate Matter Data Using Positive Matrix Factoriza-

tion?: Review of Existing Methods, J. Air Waste Manage., 57, 146–154, 2007.

Saarikoski, S., Timonen, H., Saarnio, K., Aurela, M., Järvi, L., Keronen, P., Kerminen, V.-M., and Hillamo, R.: Sources of organic carbon in fine particulate matter in northern European urban air, Atmos. Chem. Phys., 8, 6281–6295, https://doi.org/10.5194/acp-8-6281-2008, 2008.

Schell, B., Ackermann, I. J., Hass, H., Binkowski, F. S., and Ebel, A.: Modeling the formation of secondary organic aerosol within a comprehensive air quality model system, J. Geophys. Res.-Atmos., 106, 28275–28293, https://doi.org/10.1029/2001JD000384, 2001.

Shen, R. R., Schäfer, K., Schnelle-Kreis, J., Shao, L. Y., Norra, S., Kramar, U., Michalke, B., Abbaszade, G., Streibel, T., Fricker, M., Chen, Y., Zimmermann, R., Emeis, S., and Schmid, H. P.: Characteristics and sources of PM in seasonal perspective – A case study from one year continuously sampling in Beijing, Atmos. Pollut. Res., 7, 235–248, https://doi.org/10.1016/j.apr.2015.09.008, 2016.

Singh, A., Rastogi, N., Patel, A., and Singh, D.: Seasonality in size-segregated ionic composition of ambient particulate pollutants over the Indo-Gangetic Plain: Source apportionment using PMF, Environ. Pollut., 219, 906–915, 1–10, https://doi.org/10.1016/j.envpol.2016.09.010, 2016.

Sun, Y., Jiang, Q., Wang, Z., Fu, P., Li, J., Yang, T., and Yin, Y.: Investigation of the sources and evolution processes of severe haze pollution in Beijing in January 2013, J. Geophys. Res., 119, 4380–4398, https://doi.org/10.1002/2014JD021641, 2014.

Sun, Y. L., Zhuang, G. S., Huang, K., Li, J., Wang, Q. Z., Wang, Y., Lin, Y. F., Fu, J. S., Zhang, W. J., Tang, A. H., and Zhao, X. J.: Asian dust over northern China and its impact on the downstream aerosol chemistry in 2004, J. Geophys. Res.-Atmos., 115, 1–16, https://doi.org/10.1029/2009JD012757, 2010.

Sun, Y. L., Wang, Z. F., Fu, P. Q., Yang, T., Jiang, Q., Dong, H. B., Li, J., and Jia, J. J.: Aerosol composition, sources and processes during wintertime in Beijing, China, Atmos. Chem. Phys., 13, 4577–4592, https://doi.org/10.5194/acp-13-4577-2013, 2013.

Sun, Y. L., Jiang, Q., Xu, Y. S., Ma, Y., Zhang, Y. J., Liu, X. G., Li, W. J., Li, J., Wang, P. C., Wang, F., and Li, Z. Q.: Aerosol characterization over the North China Plain: Haze life cycle and biomass burning impacts in summer, J. Geophys. Res.-Atmos. Res., 121, 2508–2521, https://doi.org/10.1002/2015JD024261, 2016.

Tang, G., Zhu, X., Hu, B., Xin, J., Wang, L., Münkel, C., Mao, G., and Wang, Y.: Impact of emission controls on air quality in Beijing during APEC 2014: Lidar ceilometer observations, Atmos. Chem. Phys., 15, 12667–12680, https://doi.org/10.5194/acp-15-12667-2015, 2015.

Tang, G. Q., Sun, J., Wu, F. K., Sun, Y., Zhu, X. W., Geng, Y. J., and Wang, Y. S.: Organic composition of gasoline and its potential effects on air pollution in North China, Sci. Ser. B, 58, 1416–1425, https://doi.org/10.1007/s11426-015-5464-0, 2015.

Tang, G. Q., Zhang, J. Q., Zhu, X. W., Song, T., Münkel, C., Hu, B., Schäfer, K., Liu, Z., Zhang, J. K., Wang, L. L., Xin, J. Y., Suppan, P., and Wang, Y. S.: Mixing layer height and its implications for air pollution over Beijing, China, Atmos. Chem. Phys., 16, 2459–2475, https://doi.org/10.5194/acp-16-2459-2016, 2016a.

Tang, G. Q., Chao, N., Wang, Y. S., and Chen, J. S.: Vehicular emissions in China in 2006 and 2010, J. Environ. Sci., 48, 179–192, https://doi.org/10.1016/j.jes.2016.01.031, 2016b.

Tang, G. Q., Zhao, P. S., Wang, Y. H., Gao, W. K., Cheng, M. T., Xin, J. Y., Li, X., and Wang, Y. S.: Mortality and air pollution in Beijing: The long-term relationship, Atmos. Environ., 150, 238–243, https://doi.org/10.1016/j.atmosenv.2016.11.045, 2017.

Tao, J., Zhang, L. M., Cao, J. J., Hsu, S. C., Xia, X. G., Zhang, Z., Lin, Z. J., Cheng, T. T., and Zhang, R. J.: Characterization and source apportionment of aerosol light extinction in Chengdu, southwest China, Atmos. Environ., 95, 552–562, https://doi.org/10.1016/j.atmosenv.2014.07.017, 2014.

Tao, M., Chen, L., Xiong, X., Zhang, M., Ma, P., Tao, J., and Wang, Z.: Formation process of the widespread extreme haze pollution over northern China in January 2013: Implications for regional air quality and climate, Atmos. Environ., 98, 417–425, https://doi.org/10.1016/j.atmosenv.2014.09.026, 2014b

Tao, M. H., Chen, L. F., Su, L., and Tao, J. H.: Satellite observation of regional haze pollution over the North China Plain, J. Geophys. Res.-Atmos., 117, D12203, https://doi.org/10.1029/2012JD017915, 2012.

Tian, S. L., Pan, Y. P., and Wang, Y. S.: Size-resolved source apportionment of particulate matter in urban Beijing during haze and non-haze episodes, Atmos. Chem. Phys., 16, 1–19, https://doi.org/10.5194/acp-16-1-2016, 2016.

Turpin, B. J. and Lim, H.: Species Contributions to PM2.5 Mass Concentrations: Revisiting Common Assumptions for Estimating Organic Mass, Aerosol Sci. Technol., 35, 602–610, https://doi.org/10.1080/02786820119445, 2001.

U.S. Environmental Protection Agency: EPA Positive M atrix Factorization (PMF) 5.0 Fundamentals and User Guide, 2014.

Wang, G., Cheng, S. Y., Li, J. B., Lang, J. L., Wen, W., Yang, X. W., and Tian, L.: Source apportionment and seasonal variation of PM2.5 carbonaceous aerosol in the Beijing-Tianjin-Hebei region of China, Environ. Monit. Assess, 187, 143, https://doi.org/10.1007/s10661-015-4288-x, 2015.

Wang, G., Zhang, R., Gomez, M. E., Yang, L., Levy Zamora, M., Hu, M., Lin, Y., Peng, J., Guo, S., Meng, J., Li, J., Cheng, C., Hu, T., Ren, Y., Wang, Y., Gao, J., Cao, J., An, Z., Zhou, W., Li, G., Wang, J., Tian, P., Marrero-Ortiz, W., Secrest, J., Du, Z., Zheng, J., Shang, D., Zeng, L., Shao, M., Wang, W., Huang, Y., Wang, Y., Zhu, Y., Li, Y., Hu, J., Pan, B., Cai, L., Cheng, Y., Ji, Y., Zhang, F., Rosenfeld, D., Liss, P. S., Duce, R. A., Kolb, C. E., and Molina, M. J.: Persistent sulfate formation from London Fog to Chinese haze, P. Natl. Acad. Sci. USA, 113, 13630–13635, https://doi.org/10.1073/pnas.1616540113, 2016.

Wang, G. H., Zhou, B. H., Cheng, C. L., Cao, J. J., Li, J. J., Meng, J. J., Tao, J., Zhang, R. J., and Fu, P. Q.: Impact of Gobi desert dust on aerosol chemistry of Xi'an, inland China during spring 2009: differences in composition and size distribution between the urban ground surface and the mountain atmosphere, Atmos. Chem. Phys., 13, 819–835, https://doi.org/10.5194/acp-13-819-2013, 2013.

Wang, J., Pan, Y. P., Tian, S. L., Chen, X., Wang, L., and Wang, Y. S.: Size distributions and health risks of particulate trace elements in rural areas in northeastern China, Atmos. Res., 168, 191–204, https://doi.org/10.1016/j.atmosres.2015.08.019, 2016.

Wang, L. T., Xu, J., Yang, J., Zhao, X. J., Wei, W., Cheng, D. D., Pan, X. M., and Su, J.: Understanding

haze pollution over the southern Hebei area of China using the CMAQ model, Atmos. Environ., 56, 69–79, https://doi.org/10.1016/j.atmosenv.2012.04.013, 2012.

Wang, L. T., Wei, Z., Yang, J., Zhang, Y., Zhang, F. F., Su, J., Meng, C. C., and Zhang, Q.: The 2013 severe haze over southern Hebei, China: Model evaluation, source apportionment, and policy implications, Atmos. Chem. Phys., 14, 3151–3173, https://doi.org/10.5194/acp-14-3151-2014, 2014.

Wang, X. F., Wang, W. X., Yang, L. X., Gao, X. M., Nie, W., Yu, Y. C., Xu, P. J., Zhou, Y., and Wang, Z.: The secondary formation of inorganic aerosols in the droplet mode through heterogeneous aqueous reactions under haze conditions, Atmos. Environ., 63, 68–76, https://doi.org/10.1016/j.atmosenv.2012.09.029, 2012.

Wang, Y., Yao, L., Wang, L., Liu, Z., Ji, D., Tang, G., Zhang, J., Sun, Y., Hu, B., and Xin, J.: Mechanism for the formation of the January 2013 heavy haze pollution episode over central and eastern China, Sci. China Ser. D, 57, 14–25, https://doi.org/10.1007/s11430-013-4773-4, 2013.

Wang, Y., Bao, S., Wang, S., Hu, Y., Shi, X., Wang, J., Zhao, B., Jiang, J., Zheng, M., Wu, M., Russell, A. G., Wang, Y., and Hao, J.: Local and regional contributions to fine particulate matter in Beijing during heavy haze episodes, Sci. Total Environ., 580, 283–296, https://doi.org/10.1016/j.scitotenv.2016.12.127, 2017.

Wang, Y. H., Liu, Z. R., Zhang, J. K., Hu, B., Ji, D. S., Yu, Y. C., and Wang, Y. S.: Aerosol physicochemical properties and implications for visibility during an intense haze episode during winter in Beijing, Atmos. Chem. Phys., 15, 3205–3215, https://doi.org/10.5194/acp-15-3205-2015, 2015.

Wang, Y. S., Yao, L., Wang, L. L., Liu, Z. R., Ji, D. S., Tang, G. Q., Zhang, J. K., Sun, Y., Hu, B., and Xin, J. Y.: Mechanism for the formation of the January 2013 heavy haze pollution episode over central and eastern China, Sci. China Ser. D, 57, 14–25, https://doi.org/10.1007/s11430-013-4773-4, 2014.

Watson, J. G., Chow, J. C., and Houck, J. E.: PM2.5 chemical source profiles for vehicle exhaust, vegetative burning, geological material, and coal burning in Northwestern Colorado during 1995, Chemosphere, 43, 1141–1151, https://doi.org/10.1016/S0045-6535(00)00171-5, 2001.

Wedepohl, K. H.: The composition of the continental crust, Geochim. Cosmochim. Ac., 59, 1217–1232, 1995.

Wu, D., Mao, J. T., Deng, X. J., Tie, X. X., Zhang, Y. H., Zeng, L. M., Li, F., Tan, H. B., Bi, X. Y., Huang, X. Y., Chen, J., and Deng, T.: Black carbon aerosols and their radiative properties in the Pearl River Delta region, Sci. China Ser. D, 52, 1152–1163, https://doi.org/10.1007/s11430-009-0115-y, 2009.

Wu, R., Dai, H. C., Geng, Y., Xie, Y., Masui, T., Liu, Z. Q., and Qian, Y. Y.: Economic Impacts from PM2.5 Pollution-Related Health Effects: A Case Study in Shanghai, Environ. Sci. Technol., 51, 5035–5042, https://doi.org/10.1021/acs.est.7b00026, 2017.

Wu, S., Deng, F., Wei, H., Huang, J., Wang, X., Hao, Y., Zheng, C., Qin, Y., Lv, H., Shima, M., and Guo, X.: Association of cardiopulmonary health effects with source-appointed ambient fine particulate in Beijing, China: A combined analysis from the healthy volunteer natural relocation (HVNR) study, Environ. Sci. Technol., 48, 3438–3448, https://doi.org/10.1021/es404778w, 2014.

Xie, M., Piedrahita, R., Dutton, S. J., Milford, J. B., Hemann, J. G., Peel, J. L., Miller, S. L., Kim, S. Y., Vedal, S., Sheppard,

L., and Hannigan, M. P.: Positive matrix factorization of a 32-month series of daily PM2.5 speciation data with incorporation of temperature stratification, Atmos. Environ., 65, 11–20, https://doi.org/10.1016/j.atmosenv.2012.09.034, 2013a.

Xie, M., Barsanti, K. C., Hannigan, M. P., Dutton, S. J., and Vedal, S.: Positive matrix factorization of PM2.5 – eliminating the effects of gas/particle partitioning of semivolatile organic compounds, Atmos. Chem. Phys., 13, 7381–7393, https://doi.org/10.5194/acp-13-7381-2013, 2013b.

Xin, J., Wang, Y., Pan, Y., Ji, D., Liu, Z., Wen, T., Wang, Y., Li, X., Sun, Y., Sun, J., Wang, P., Wang, G., Wang, X., Cong, Z., Song, T., Hu, B., Wang, L., Tang, G., Gao, W., Guo, Y., Miao, H., Tian, S., and Wang, L.: The campaign on atmospheric aerosol research network of China: CARE-China, B. Am. Meteorol. Soc., 96, 1137–1155, https://doi.org/10.1175/BAMS-D-14-00039.1, 2015.

Xu, W. Y., Zhao, C. S., Ran, L., Deng, Z. Z., Liu, P. F., Ma, N., Lin, W. L., Xu, X. B., Yan, P., He, X., Yu, J., Liang, W. D., and Chen, L. L.: Characteristics of pollutants and their correlation to meteorological conditions at a suburban site in the North China Plain, Atmos. Chem. Phys., 11, 4353–4369, https://doi.org/10.5194/acp-11-4353-2011, 2011.

Yang, L. X., Zhou, X. H., Wang, Z., Zhou, Y., Cheng, S. H., Xu, P. J., Gao, X. M., Nie, W., Wang, X. F., and Wang, W. X.: Airborne fine particulate pollution in Jinan, China: Concentrations, chemical compositions and influence on visibility impairment, Atmos. Environ., 55, 506–514, https://doi.org/10.1016/j.atmosenv.2012.02.029, 2012.

Yang, Y. R., Liu, X. G., Qu, Y., An, J. L., Jiang, R., Zhang, Y. H., Sun, Y. L., Wu, Z. J., Zhang, F., Xu, W. Q., and Ma, Q. X.: Characteristics and formation mechanism of continuous hazes in China: A case study during the autumn of 2014 in the North China Plain, Atmos. Chem. Phys., 15, 8165–8178, https://doi.org/10.5194/acp-15-8165-2015, 2015.

Ying, Q., Wu, L., and Zhang, H. L.: Local and inter-regional contributions to PM2.5 nitrate and sulfate in China, Atmos. Environ., 94, 582–592, https://doi.org/10.1016/j.atmosenv.2014.05.078, 2014.

Yuan, B., Liu, Y., Shao, M., Lu, S. H., and Streets, D. G.: Biomass burning contributions to ambient VOCs species at a receptor site in the Pearl River delta (PRD), China, Environ. Sci. Technol., 44, 4577–4582, https://doi.org/10.1021/es1003389, 2010.

Zhang, J. K., Sun, Y., Liu, Z. R., Ji, D. S., Hu, B., Liu, Q., and Wang, Y. S.: Characterization of submicron aerosols during a month of serious pollution in Beijing, 2013, Atmos. Chem. Phys., 14, 2887–2903, https://doi.org/10.5194/acp-14-2887-2014, 2014.

Zhang, J. K., Wang, Y. S., Huang, X. J., Liu, Z. R., Ji, D. S., and Sun, Y.: Characterization of Organic Aerosols in Beijing Using an Aerodyne High-Resolution Aerosol Mass Spectrometer, Adv. Atmos. Sci., 32, 877–888, https://doi.org/10.1007/s00376-014-4153-9, 2015.

Zhang, J. K., Wang, L. L., Wang, Y. H., and Wang, Y. S.: Submicron aerosols during the Beijing Asia-Pacific Economic Cooperation conference in 2014, Atmos. Environ., 124, 224–231, https://doi.org/10.1016/j.atmosenv.2015.06.049, 2016.

Zhang, K., Batterman, S., and Dion, F.: Vehicle emissions in congestion: Comparison of work zone, rush hour and free-flow conditions, Atmos. Environ., 45, 1929–1939, https://doi.org/10.1016/j.atmosenv.2011.01.030, 2011.

Zhang, R., Jing, J., Tao, J., Hsu, S. C., Wang, G., Cao, J., Lee, C. S. L., Zhu, L., Chen, Z., Zhao, Y., and Shen, Z.: Chemical characterization and source apportionment of PM2.5 in Beijing: seasonal perspective, Atmos. Chem. Phys., 13, 7053–7074, https://doi.org/10.5194/acp-13-7053-2013, 2013.

Zhang, R. Y., Wang, G. H., Guo, S., Zamora, M. L., Ying, Q., Lin, Y., Wang, W. gang, Hu, M., and Wang, Y.: Formation of urban fine particulate matter, Chem. Rev., 115, 3803–3855, https://doi.org/10.1021/acs.chemrev.5b00067, 2015.

Zhang, X. Y., Wang, Y. Q., Niu, T., Zhang, X. C., Gong, S. L., Zhang, Y. M., and Sun, J. Y.: Atmospheric aerosol compositions in China: spatial/temporal variability, chemical signature, regional haze distribution and comparisons with global aerosols, Atmos. Chem. Phys., 12, 779–799, https://doi.org/10.5194/acp-12-779-2012, 2012.

Zhang, Y. J., Zheng, M., Cai, J., Yan, C. Q., Hu, Y. T., Russell, A. G., Wang, X. S., Wang, S. X., and Zhang, Y. H.: Comparison and overview of PM2.5 source apportionment methods, Chinese Sci. Bull., 60, 109–121, https://doi.org/10.1360/n972014-00975, 2015.

Zhang, Y. L. and Cao, F.: Fine particulate matter (PM 2.5) in China at a city level, Sci. Rep., 5, 14884, https://doi.org/10.1038/srep14884, 2015.

Zhao, B., Wang, P., Ma, J. Z., Zhu, S., Pozzer, A., and Li, W.: A high-resolution emission inventory of primary pollutants for the Huabei region, China, Atmos. Chem. Phys., 12, 481–501, https://doi.org/10.5194/acp-12-481-2012, 2012.

Zhao, P. S., Dong, F., Yang, Y. D., He, D., Zhao, X. J., Zhang, W. Z., Yao, Q., and Liu, H. Y.: Characteristics of carbonaceous aerosol in the region of Beijing, Tianjin, and Hebei, China, Atmos. Environ., 71, 389–398, https://doi.org/10.1016/j.atmosenv.2013.02.010, 2013a.

Zhao, P. S., Dong, F., He, D., Zhao, X. J., Zhang, X. L., Zhang, W. Z., Yao, Q., and Liu, H. Y.: Characteristics of concentrations and chemical compositions for PM$_{2.5}$ in the region of Beijing, Tianjin, and Hebei, China, Atmos. Chem. Phys., 13, 4631–4644, https://doi.org/10.5194/acp-13-4631-2013, 2013b.

Zhao, P. S., Dong, F., He, D., Zhao, X. J., Zhang, X. L., Zhang, W. Z., Yao, Q., and Liu, H. Y.: Characteristics of concentrations and chemical compositions for PM$_{2.5}$ in the region of Beijing, Tianjin, and Hebei, China, Atmos. Chem. Phys., 13, 4631–4644, https://doi.org/10.5194/acp-13-4631-2013, 2013c.

Zhao, X. J., Zhang, X. L., Xu, X. F., Xu, J., Meng, W., and Pu, W. W.: Seasonal and diurnal variations of ambient PM2.5 concentration in urban and rural environments in Beijing, Atmos. Environ., 43, 2893–2900, https://doi.org/10.1016/j.atmosenv.2009.03.009, 2009.

Zhao, X. J., Zhao, P. S., Xu, J., Meng, W., Pu, W. W., Dong, F., He, D., and Shi, Q. F.: Analysis of a winter regional haze event and its formation mechanism in the North China Plain, Atmos. Chem. Phys., 13, 5685–5696, https://doi.org/10.5194/acp-13-5685-2013, 2013.

Zhu, X., Tang, G., Hu, B., Wang, L., Xin, J., Zhang, J., Liu, Z., Münkel, C., and Wang, Y.: Regional pollution and its formation mechanism over North China Plain: A case study with ceilometer observations and model simulations, J. Geophys. Res.-Atmos., 121, 14574–14588, https://doi.org/10.1002/2016JD025730, 2016.

Zong, Z., Wang, X. P., Tian, C. G., Chen, Y. J., Qu, L., Ji, L., Zhi, G. R., Li, J., and Zhang, G.: Source apportionment of PM$_{2.5}$ at a regional background site in North China using PMF linked with radiocarbon analysis: Insight into the contribution of biomass burning, Atmos. Chem. Phys., 16, 11249–11265, https://doi.org/10.5194/acp-16-11249-2016, 2016.